Journal of Archaeological Science: Reports 63 (2025) 105080

Contents lists available at ScienceDirect

Journal of Archaeological Science: Reports

journal homepage: www.elsevier.com/locate/jasrep

Revisiting the thermal alteration of buried bone☆

Giulia Gallo [a,b,c,*], Vera Aldeias [d], Mareike Stahlschmidt [e,f,g]

[a] Anthropology Department, University California Davis, United States
[b] TRACES Laboratoire, Université Toulouse Jean Jaurès, Toulouse, France
[c] Chair of Paleoanthropology, CIRB (UMR 7241–U1050), Collège de France, Paris, France
[d] ICArEHB - Interdisciplinary Center for Archaeology and the Evolution of Human Behaviour, Universidade do Algarve, Faro, Portugal
[e] Former Department of Human Evolution, Max Planck Institute for Evolutionary Anthropology, Leipzig, Germany
[f] Human Evolution and Archaeological Sciences (HEAS), University of Vienna, Vienna, Austria
[g] Department of Evolutionary Anthropology, University of Vienna, Vienna, Austria

ARTICLE INFO

Keywords:
Experimental archaeology
Zooarchaeology
Bone
Burned bone
Spectroscopy
FTIR
XRD

ABSTRACT

The impacts of heat exposure directly on bone material are widely acknowledged, yet a comprehensive understanding regarding the degree of thermal alteration experienced by bone buried beneath a combustion feature or fire event remains poorly described. Such potential incidental burning below a surface fire presents challenges for distinguishing between the intentional remains of fire use behaviors from haphazard heat exposure. In this study, we address the extent to which buried bone material can undergo alteration under concentrated high-heat conditions, achieved through using a fire simulator operating at 950 °C for a duration of 6 h simulating a high temperature hearth fire. Here we describe the degree of carbonization and calcination in bone samples buried at three depths (−2, −6, and −10 cm) in gravel and a mixed gravel and fine sand substrate. We find that, at the sustained temperature of 950 °C, plus heating and cooling time, calcination of bone material can occur at shallow depths of −2 cm under the fire simulator, whereas at −6 cm only one sample of each experimental condition is recognized to be fully structurally and chemically calcined. Despite only two samples calcining at this depth, several other bones buried at −6 cm displayed pale and light coloration, experiencing the elimination of organics without undergoing true calcination, likely due to the prolonged exposure to heat removing the organic component. At −10 cm depth, bone material centered under the heat source became carbonized, while buried bones positioned at the periphery of the heat source are recognized only be partially thermally altered. Notably, neither gravel nor a mixture of gravel and sand substrates create a detectable reduction environment in the spectroscopic analyses of the buried bones. Our findings highlight that not only can post-depositional heating significantly impact buried faunal material, but that in this way humans can act as post-depositional agents.

1. Introduction

Fire is hypothesized to have played a significant and complex role in hominin evolution (Chazan, 2017; Gowlett, 2016; Wrangham, 2009; 2017). However, distinguishing between natural fires, anthropogenic fires, and incidental thermal exposure in the archaeological record remains a significant challenge (Goldberg et al., 2017). Researchers studying combustion features must carefully avoid misinterpreting thermally altered material found beneath a heating event, which could result from incidental exposure, as intentional components of an anthropogenic feature (Aldeias et al., 2017). Such misclassification hinders questions of human behavior regarding what was purposefully included in fires, as well as the timing of the fire event.

Prior studies on the thermal alteration of buried bone demonstrate that heat transfer from surface combustion features can impact buried materials, but there are significant variations in findings due to differences in experimental designs (including outdoors vs. laboratory), the inclusion of bone of different states (e.g., fresh or dry modern bone and/or archaeological bone), fire durations, temperatures, and analytical methods (SI Table 1; Bennett, 1999; De Graaff, 1961; Stiner et al., 1995, Tellez et al., 2022). Some studies report calcination (indicating temperature alteration in oxygen atmospheres > ~680 °C) in bone buried underneath combustion features (SI Table 1; Bennett, 1999; Tellez et al., 2022). However, these observations are often based on macroscopic

☆ This article is part of a special issue entitled: 'Experimental Arch-Animals' published in Journal of Archaeological Science: Reports.

* Corresponding author at: Department of Anthropology, University of California, Davis, One Shields Avenue, Davis, California 95616 USA.
E-mail address: gtgallo@ucdavis.edu (G. Gallo).

https://doi.org/10.1016/j.jasrep.2025.105080
Received 30 September 2024; Received in revised form 7 February 2025; Accepted 3 March 2025
Available online 13 March 2025

evaluations, such as color and texture, rather than spectroscopic data. Spectroscopic analysis is critical for verifying chemical and structural changes in bone mineral, as depigmentation—the removal of organic char—can occur from prolonged exposure to lower temperatures, not just high temperatures (Gallo et al., 2023). Notably, only one prior study (Stiner et al., 1995) includes spectroscopic data. Given the varying results and reported data of prior studies, highly controlled and reproducible experimental conditions are essential for contextualizing the previous research and for establishing robust frameworks applicable to archaeological data.

1.1. Thermal impact on buried substrates

Prior research has assessed the impact of heat transfer onto underlying sediments (for review see Aldeias et al., 2016). Bellomo (1990) conducted extensive research on observed campfires, stump fire, and grass fire experiments in Kenya and the USA (Illinois) on different soil types, noting that subsurface temperatures diminish with depth. This study found that the average soil temperatures at −1 cm depth typically ranged from 175-475 °C, while at −5 cm were seen to reach 100–230 °C (Bellomo, 1990; Canti and Linford, 2000). Canti and Linford (2000) highlight the complexities of understanding thermal impacts on soils beneath fires, emphasizing the highly variable nature of heat transfer and hypothesizing that the interacting factors like substrate composition, compaction, and environmental conditions interact considerably with the experienced temperatures above and below ground. This study recorded wood-fueled fires monitored between 4–6 h and observed maximum above ground temperatures spanning 818–995 °C and soil temperatures displaying significant variation at −1 cm (433–570 °C) and −4 cm depths (199–318 °C; Canti and Lindford, 2000). These findings underscore the challenges in predicting subsurface heating, even under known conditions, due to the interplay of multiple dynamic factors.

A controlled laboratory experiment utilizing a fire simulator setup presented in Aldeias et al. (2016) has tested the extent of surface heating on several variable subsurface conditions, including grain size and mineralogy, degree of compaction, as well as moisture content at temperature thresholds of 600 and 950 °C for 6 h, 9 h, 19 h, and in stepping durations. Results of this study highlight that heat from combustion features at these durations and sustained temperatures can reach underlying deposits to degrees which impact both the substrates as well as any objects buried within that sediment, even at depths of – 10 cm (Aldeias et al., 2016). In these experimental setups, the presence of moisture was found to hinder heat transfer (Aldeias et al., 2016). This occurs because the thermal energy converts water into gas, which slows down the process of heat exchange. This effect was also noted for when heat interacted with water in organic matter, although the combustion of shallowly buried organic materials themselves can also became a source of heat (Aldeias et al., 2016). The compaction of underlying sediment is also seen to increase the rate of heat transfer beneath a fire, as compaction eliminates insulating air voids (Aldeias et al., 2016). In terms of the vertical distribution of heat, as depth increased, Aldeias et al. (2016) documented a decrease in the rate of the temperature ramp as heat transfer gradually slowed. In this experiment, the maximum temperatures achieved in all experimental setups were found to be correlated to both the intensity of the programmed heat and the duration for which the temperature was maintained as lower depths gradually rose to eventual thermal equilibrium (Aldeias et al., 2016).

Between the different sediments, notable temperature disparities exceeding 50 °C were observed at −2 cm, but temperature variations were minimal at greater depths (Aldeias et al., 2016). Within the experiments it was also consistently noted that after the fire simulator furnace was powered off, the temperature did continue to rise at the deepest points monitored by thermocouples, demonstrating the heat retention of the buried substrates (Aldeias et al., 2016). Aldeias et al. (2016) further tested the lateral distribution of heat adjacent to the opening of the fire simulator and found that the areas proximate to the emitted heat did not reach the intensities seen directly under the furnace.

Overall, however, it is important to note that differences in temperatures observed between laboratory and field experiments may arise from the potential greater directionality of heat in a furnace-based setup. A laboratory furnace likely yields a more focused and consistent heat flow compared to an active outdoor fire, which is interacting with the surrounding atmosphere, wind, and generating a radiative heat that can be drawn upward rather than concentrated downward. Nonetheless, laboratory experiments remain valuable for isolating and understanding the basic dynamics and variables of heat transfer, allowing for a controlled assessment of these processes.

1.2. Transformations to bone material when exposed to heat

An extensive body of research has established the transformative effects of thermal exposure on osseous materials under varying conditions of temperature, duration, and atmosphere. These studies underscore the value of thermally altered bone in forensic and archaeological analyses (Ellingham et al., 2015; Mamede et al., 2018a; Mayne Correia, 1997; Etok et al., 2007; Reidsma et al., 2016; Reidsma, 2022; Van Hoesel et al., 2019; Marques et al., 2021; Shehata and Krap, 2024; Snoeck et al., 2016; Thompson, 2004; Zazzo et al., 2009). Bone's primary components—collagen, bioapatite, and water (Martin et al., 2015)—are impacted by heat exposure, with the elimination of water and collagen occurring at lower thermal thresholds. Changes in the composition and crystallinity of bioapatite at higher temperatures are particularly diagnostic of different thermal conditions (for review, see SI 'Review on the thermal alteration of bone'; Drouet et al., 2018; Mamede et al., 2018; Marques et al., 2021; Reidsma et al., 2016; Reidsma, 2022; Rey et al., 2009; Shehata and Krap, 2024; Van Hoesel et al., 2019).

Thermal modification of bone typically involves dehydration, organic decomposition, carbonate elimination, and the transformation of bioapatite into more crystalline forms with higher stoichiometry occurring at temperatures of ~ 680 °C or higher when under oxidizing conditions, a process known as calcination (Ellingham et al., 2015; Gallo et al., 2021, 2023; Shehata and Krap, 2024). Ultimately, with sustained high temperatures over approximately 1000 °C it is possible to produce α- (α-TCP) and β-tricalcium phosphate (β-TCP) (Gibson et al., 2000; Piga et al., 2018; Shehata and Krap, 2024).

The coloration of burned bones are influenced by atmospheric conditions and heating duration and do not always correlate neatly with temperature exposure. The organic char responsible for dark coloration in bones which combust at low temperatures (~300 °C) and in oxidizing conditions can still be removed through long duration periods, and do not necessarily need high temperatures to be eliminated (Gallo et al. 2023). This results in bones burned at low temperatures but for long periods having similar pale white and gray colorations usually associated with calcination at higher temperatures (~600–700 °C +) in an aerobic atmosphere (Gallo et al. 2023). In shorter durations but under reducing conditions, however, the organics are not combusted, and a dark, black coloration remains even at higher temperatures with the formation of amorphous carbon (Reidsma et al., 2016; Marques et al.; 2021). These discrepancies in coloration reflective of different burning environments and properties, and highlights the necessity of verifying visual temperature threshold assessments with spectroscopic analyses to evaluate structural and chemical changes. These changes can be observed macroscopically through color and texture alterations, can be distinguished from burial environment staining, and can be confirmed through spectroscopic methods like FTIR (Fourier Transform Infrared Spectroscopy), which assess crystallinity and chemical composition (Bradfield, 2018; Dupras and Schultz, 2014; Gallo et al., 2021, 2023; Mamede et al., 2018a; Pollock et al., 2018; Shahack-Gross et al., 1997; Turner et al., 2018; Weiner and Bar-Yosef, 1990; Piga et al., 2018). X-ray diffraction (XRD) further supports these analyses by providing direct

measurements of the average crystallite size to complement the FTIR ratios, which can be biased at higher temperatures (Ellingham et al., 2015; Gallo et al., 2021, 2023).

In this paper, we examine the thermal impact on buried bone through two experimental conditions conducted in controlled laboratory settings with bones of standardized freshness and size. These setups were designed to complement the work of Aldeias et al. (2016) for comparability with previously tested heating conditions in differing sediment substrates. The high temperature (950 °C) and duration time (6 h) were intentionally selected to provide a controlled baseline. We acknowledge that these conditions represent the upper limit of what can realistically be produced by anthropogenic fire and exceeds the likely temperatures and durations of typical hunter-gatherer fires (Aldeias et al. 2017; Bellomo 1993, 1994; Black and Thoms 2014; Friesem et al., 2017; Gowlett et al. 1981, 2017; Mallol et al., 2017), but testing this high-intensity allows us to better understand the maximum range of possible thermal damage. From this and prior research on temperature distributions in sediments, we can extrapolate the effects to bone at lower temperatures. We additionally tested two dry sediment compositions to assess differences in oxygen availability beneath combustion features.

We do note that these results are based on an indoor furnace experiment and may not be directly translatable to outdoor fires on varying sediment substrates, where factors such as airflow, sediment composition and moisture content, fuel types, and fire dynamics may differ the directionality and sustained intensity of thermal emittance. But by clearly defining and controlling the experimental variables selected here, we aim to provide a clearer understanding of how they interact to cause alteration in bone, thereby informing our understanding of thermal damage possible to be observed in archaeological contexts.

The objectives of this paper are to address:

A) How does burial depth affect the amount of temperature exposure subsurface bones experience?
B) What role does the proximity to the center of the heat source play in the temperature exposure of subsurface bone?
C) How does sediment composition with different grain sizes influence the transfer of heat as well as the access to oxygen?

2. Methods & materials

2.1. Bone procurement

Diaphyseal shafts entirely of cortical tissue from bovid (*Bos taurus*) femurs and humeri diaphyses were obtained from a local butcher (Fleischerei Englen, Leipzig, Germany) from six different elements (SI 'Research design for experimental study engaging with animal materials'). Bones were defleshed the same morning as purchased. After marrow removal, each element was subsequently cut into a minimum of twelve approximately 2 cm cubic squares using an electric floor bolted large animal veterinary bone saw (Fleischerbandsaege) with a fixed worktable at the Veterinar-Anatomisches Institut- VMF (Leipzig, Germany; SI Figs. 1 and 2; SI Tables 2–5). Bones were utilized in both experimental conditions within two days of purchase and were stored between setups in saline soaked gauze wraps (Braun NaCl 0.9 %) refrigerated at temperatures averaging 4 °C to maintain a hydrated state comparable to fresh bone (Zhang et al., 2018).

In both experimental conditions, bone fragments were collected from each cut element (diaphyseal shafts of bones labeled M, N, O, R, P, and Q) without adhering to specific selection criteria. To avoid consistent burial positions or orientations of bones from the same element, the arrangement of bones from the same diaphysis were alternated in each experimental setup (SI Table 6). Each experiment included no more than two fragments from the same diaphysis, with samples distinguished by subscripts 'a' or 'b' for identification (e.g., Xa, Xb representing two fragments from bone X).

2.2. Experimental design

The experimental parameters were selected to replicate the maximum heat transfer observed in Aldeias et al. (2016), with our objective to subject the samples to significant thermal alteration as predicted by the previous experiments. The elevated temperatures were also chosen to test intensive conditions relevant for understanding the maximum extents of thermal alteration of subsurface buried bone, while the long duration period was desired to allow for the heat to sufficiently impact the sediments at −10 cm. These limits were further chosen to replicate temperatures and lengths that were elevated and significant but not impossible for pre-industrial archaeological fires.

We aim here to establish a reference dataset created in reproducible conditions to serve as a foundation for further studies enhancing our understanding of the thermal alteration of buried bone, but also to serve as a starting point to assist in extrapolating to various other fire, substrate, and bone conditions. For a detailed examination of internal, external, and ecological validity in experimental archaeology, see Aldeias et al. (2016). For a discussion of standardization practices and ethical considerations in zooarchaeology, refer to Steele et al. (2025, this issue).

We used a high-temperature electric heater (Micropyretics Heater International) to control the duration and temperature of the heating event following Aldeias et al. (2016). The heater apparatus was suspended on a frame directly above a wooden box with a minimal air gap between the furnace and the substrate surface (Aldeias et al., 2016). The suspended furnace emitted radiation heat in two experiments using different substrates: a mixture of gravel, grain size 2–4 mm, and fine mineral sand. 0.1–0.4 mm (Fire Simulation setup 1 'FS1′), and gravel alone (Fire Simulation setup 2 'FS2′; Fig. 1). The purpose of a mix of gravel and fine sand for the first experimental setup was to test the conductivity of a substrate composed of two grain sizes. All substrates utilized in both experimental conditions were air dried prior to filling the wooden basin.

Twelve bone segments were positioned across three levels within each matrix at depths of −2, −6, and −10 cm. Position of the arrangement was determined by measurements from the box edges to ensure a central position. Clusters at each depth were arranged in four rows of three, each spaced approximately 3–4 cm from the closest neighbor, with the first and last row designated as 'peripheral', as they were the closest to the edges of the furnace footprint (approximately 20 cm in diameter), while the center two rows considered more centrally placed under the furnace, or 'central' (Fig. 1). Four pieces of ostrich eggshell were also burned at each depth for a different experiment (SI Figs. 4–18), but their analysis is not included in this study.

In addition to the internal display of the instrument representing the thermal output of the furnace, k-type thermocouple probes were used to monitor the temperature rate, confirm temperature stabilization, and to provide measurements of the dispersal of heat from the furnace into the substrates. These external thermocouples were placed at each depth (−2, −6, and −10 cm) and at the center of the bone arrangement as well as at the peripheral of the cluster.

Twelve additional bones were placed in a Nabertherm muffle furnace set at 950 °C for 6 h to provide a relative control sample representing bones which would be thermally altered at the surface conditions of this fire event. Our goal was to establish a comparison group that would experience the same temperature conditions as set by the furnace without any interference by depth or sediment matrix. These bones could not be placed under the fire simulator setup due to the proximity of the furnace to the substrates, and therefore a muffle furnace was used to maintain consistent and comparable temperature parameters for testing. Two bones were placed per crucible (total 6 crucibles, three per setup) resting on two substrates mimicking the Fire Simulation setups: mixed dry gravel and fine sand (Muffle Furnace Control 1, 'MF1′), and

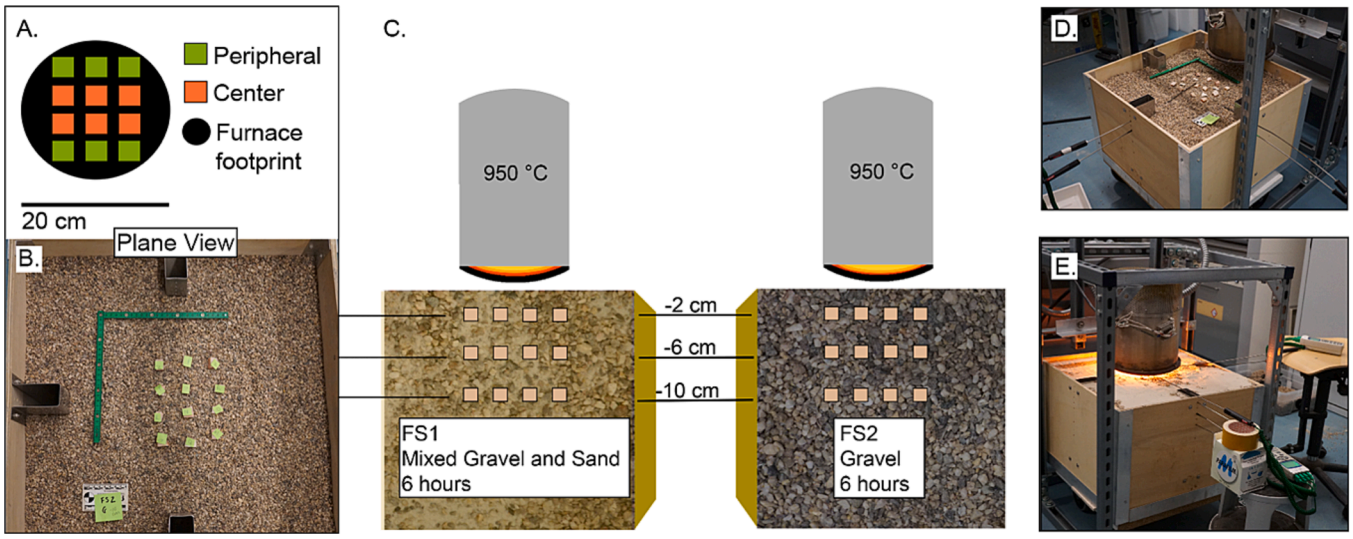

Fig. 1. Experimental setup utilized in this study. A) Bones arranged at three depths within the sediment basin, with bones closer to the edge of the furnace footprint labeled as peripheral; B) Bone fragments placed with labels prior to being covered with overlying sediment to ensure randomization and later identification; C) Two sediment substrates tested with temperature and duration held consistent; D) Thermocouple probs placed both in the center of the thermal footprint as well as resting near the edge; E) Furnace held suspended directly over sediment basin.

only dry gravel (Muffle Furnace Control 2, 'MF2'; SI Fig. 3).

2.3. Color observations and assigned burning stage

Bone color was documented on all solid fragment surfaces following experimental setups using a Color Gun RM200 CAPSURE color matching tool utilizing sensors to detect the spectral reflectance of the object to provide color readings following the Munsell Color Chart (Munsell Color, 2010). Samples were tested in several orientations with each unique color result recorded.

All bone fragments were blindly assigned a modified Stiner et al. (1995) burning stage subsequent to the heating experiments based only on visual cues of coloration and surface texture for future comparison with the spectroscopic results (Table 1). These stages are determined through macroscopic observations and cover initial carbonization or charring, full carbonization or charring, and partial and full calcination. The addition of two stages here, Stage 3D (carbonization/charring with depigmentation) and Stage D, full depigmentation, are suggested here to account for samples which have experienced an elimination of the organic component due to long durations at temperatures but have not calcined as observed in Gallo et al. (2023). Carbonization and charring cannot be distinguished visually as well, therefore prior to spectroscopic analysis dark coloration necessitates the use of both terminologies to describe black and dark brown visual cues that co-occur with thermal alteration (for further review of the processes of carbonization and charring, see Reidsma et al., 2016; Marques et al., 2021;Van Hoesel et al., 2019). Depigmentation can be visually assessed in modern experimental samples due to the presence of pale colors associated with the greys and silvers of calcination but with a more tan and/or beige muted hue and without the chalky, matte and cracked surface textures that accompany true calcination (Gallo et al., 2023). These macroscopic observations were re- checked and either confirmed or changed in case of conflicting spectroscopic results (Table 2).

Table 1
Modified Stiner et al. (1995) scale of burning intensity based on distribution patterns of carbonization/charring and calcination. Two stages have been added to allow for observations of depigmentation, which often presents with different visual cues than typically seen in carbonization or calcined bone.

Stage	Description	Reported associated coloration*
0	Not burnt	Yellow-white or tans
1	Slightly burnt, < 50 % carbonized and/or charred	< 50 % dark browns/ dark greys/ reddish browns
2	Majority burnt, > 50 % carbonized and/or charred	> 50 % dark browns/ dark greys/ reddish browns
3	Fully carbonized and/or charred	Dark browns/ dark greys/ reddish browns
3D	Presence of carbonization and/or char with presence of depigmentation	Presence of dark browns/dark greys/ reddish browns with pale beiges/ greys/tans/light browns
D	Fully depigmented	Pale beiges/greys/tans/light browns
4	Slightly highly burnt, < 50 % calcined	< 50 % greys/ grey-blues/ whites
5	Majority highly burnt, > 50 % calcined	> 50 % greys/grey-blues/whites
6	Fully calcined	White/ light greys/ grey-blue patches

* modified following Snoeck et al. (2014) and observations of depigmentation from Gallo et al. (2023).

2.4. FTIR-ATR

Portions of bone samples were ground using an agate mortar and pestle, followed by sieving with a 234-μm mesh, prior to spectroscopic analyses. The ATR attachment was chosen to minimize contamination, conduct minimally invasive testing, and to ensure comparability with prior referential datasets collected with ATR (Bruno 1999, Gallo et al., 2021, 2023; Hollund et al., 2013; Thompson et al., 2009; Nakamoto, 2009). Analyses were performed using a Nicolet 6700 Fourier transform infrared spectrometer with a single bounce diamond crystal and a deuterated triglycine (DTGS) detector. 256 scans were collected in a wavelength range of 4000–400 cm^{-1} with a sample gain of 8 and a resolution of 4 cm^{-1}.

The FTIR spectra taken for this study were not normalized or altered. This decision was made to preserve the raw data, as normalization could have introduced artificial scaling effects that might mask subtle but significant variations in the spectra, particularly those related to specific functional group changes. Instead, we focused on direct comparison of spectral features and peak intensities to assess the thermal modifications.

Five ratios and four observations from relevant general band assignments were included in this study to assess the extent of thermal alteration on these bones, including: the OH/P, CO/P, C/P, PHT, and SF ratios (Ellingham et al., 2015, Mamede et al., 2018, Thompson et al.,

Table 2
Original and modified Stiner et al. (1995) assignments per substrate and depth. Position within the bone cluster at each depth is denoted by a 'P' for peripheral or 'C' for central.

Experimental setup	Substrate	Depth (cm)	Bone ID	Primary Stage Assessment	Revised Stage Assessment	Central (C) or Peripheral (P)
FS1	Gravel and Sand	−2	Pa	3D		P
FS1	Gravel and Sand	−2	Na	D		P
FS1	Gravel and Sand	−2	Nb	3D		P
FS1	Gravel and Sand	−2	Qa	5		C
FS1	Gravel and Sand	−2	Ra	6		C
FS1	Gravel and Sand	−2	Oa	**6**	**D**	C
FS1	Gravel and Sand	−2	Pb	6		C
FS1	Gravel and Sand	−2	Ma	6		C
FS1	Gravel and Sand	−2	Qb	6		C
FS1	Gravel and Sand	−2	Mb	**5**	**D**	P
FS1	Gravel and Sand	−2	Ob	6		P
FS1	Gravel and Sand	−2	Rb	5		P
FS2	Gravel	−2	Ma	3D		P
FS2	Gravel	−2	Qa	6		P
FS2	Gravel	−2	Oa	6		P
FS2	Gravel	−2	Ob	**5**	**D**	C
FS2	Gravel	−2	Mb	6		C
FS2	Gravel	−2	Pa	6		C
FS2	Gravel	−2	Na	5		C
FS2	Gravel	−2	Nb	6		C
FS2	Gravel	−2	Ra	D		P
FS2	Gravel	−2	Rb	6		P
FS2	Gravel	−2	Pb	6		P
FS1	Gravel and Sand	−6	Na	3		P
FS1	Gravel and Sand	−6	Pa	6		P
FS1	Gravel and Sand	−6	Ma	3		P
FS1	Gravel and Sand	−6	Pb	3D		C
FS1	Gravel and Sand	−6	Oa	**5**	**D**	C
FS1	Gravel and Sand	−6	Ra	3		C
FS1	Gravel and Sand	−6	Rb	3D		C
FS1	Gravel and Sand	−6	Nb	**6**	**D**	C
FS1	Gravel and Sand	−6	Ob	3		C
FS1	Gravel and Sand	−6	Qa	**5**	**3D**	P
FS1	Gravel and Sand	−6	Qb	**6**	**D**	P
FS1	Gravel and Sand	−6	Mb	**6**	**D**	P
FS2	Gravel	−6	Pa	3		P
FS2	Gravel	−6	Na	D		P
FS2	Gravel	−6	Nb	D		P
FS2	Gravel	−6	Qa	3D		C
FS2	Gravel	−6	Ra	**6**	**D**	C
FS2	Gravel	−6	Oa	**6**	**D**	C
FS2	Gravel	−6	Pb	D		C
FS2	Gravel	−6	Ma	**6**	**D**	C
FS2	Gravel	−6	Qb	6		C
FS2	Gravel	−6	Mb	3		P
FS2	Gravel	−6	Ob	**5**	**3D**	P
FS2	Gravel	−6	Rb	3D		P
FS1	Gravel and Sand	−10	Ma	1		P
FS1	Gravel and Sand	−10	Qa	3		P
FS1	Gravel and Sand	−10	Oa	3		P
FS1	Gravel and Sand	−10	Ob	3		C
FS1	Gravel and Sand	−10	Mb	3		C
FS1	Gravel and Sand	−10	Pa	3		C
FS1	Gravel and Sand	−10	Na	2		C
FS1	Gravel and Sand	−10	Qb	3		C
FS1	Gravel and Sand	−10	Nb	3		C
FS1	Gravel and Sand	−10	Ra	2		P
FS1	Gravel and Sand	−10	Pb	2		P
FS1	Gravel and Sand	−10	Rb	3		P
FS2	Gravel	−10	Na	2		P
FS2	Gravel	−10	Pa	3		P
FS2	Gravel	−10	Ma	3		P
FS2	Gravel	−10	Pb	2		C
FS2	Gravel	−10	Oa	3		C
FS2	Gravel	−10	Ra	3		C
FS2	Gravel	−10	Rb	3		C
FS2	Gravel	−10	Nb	3		C
FS2	Gravel	−10	Ob	3		C
FS2	Gravel	−10	Qa	1		P
FS2	Gravel	−10	Qb	2		P
FS2	Gravel	−10	Mb	3		P

2013; Snoeck et al., 2014; SI Tables 7, 8). These measurements provide semi-quantitative evaluations on: 1) the relative organic content 2) the relative lattice carbonate content 3) an index of crystallinity and 4) the presence of hydroxyls which become visible at higher temperatures, and 5) the presence of peaks representing compounds relevant to heating in reduction atmospheres (SI Tables 7, 8). Notably, the absence of OH signals, along with NCN deformation and stretching modes, likely indicates thermal alteration in a reduction environment with limited oxygen access (SI Table 7; Marques et al., 2021).

2.5. XRD

Four samples from FS2 representing −2, and −6 cm depths as well as one 'surface' control sample from MF2 were selected for independent measures of average crystallite size using XRD. To obtain the peaks necessary to infer any crystallite growth, a Bruker D2 Phaser diffractometer was used with CuKx radiation. Divergent slits were placed at 0.6 mm with a 1 mm anti-scatter screen, with a maximum opening of the position sensitive detector 4.8°. Parameters of this analysis include 7 to 70° 2θ with 0.04°step and 0.02 θ increment. Zero background silicon holders were used to hold the powdered samples, which were spread evenly over the surface using ethanol. Whole pattern fitting, Rietveld refinement (Rietveld, 1969) was used to ascertain the average crystallite sizes using hydroxyapatite Ca5(PO4)3OH structure (space group P63/m) in the open access software GSAS-II (Toby and Von Dreele 2013).

2.6. Fire Simulator furnace

The FS experiments were timed for 6 h once the furnace reached 950 °C for both setups (FS1 and FS2). The ramping time for the suspended furnace to reach this maximum temperature took an average of 3 h and 45 min, resulting in a total time of heat exposure experienced by bone samples to be greater than 10 h in addition to the gradual cooling period. After the experiment, both sediment types exhibited rubified substrates indicating the placement of the furnace (Fig. 2). Rubification was observed at the surface of the sediment for both experimental setups as well as at −2 cm depth for the mixed substrates (FS1) and at −6 cm depth when only gravel was used (FS2; SI Figs. 4–22. Bones were excavated carefully and were only collected once all fragments were excavated to verify their placement (SI Figs. 4–22).

Thermocouples were strategically positioned at three depths (−2 cm, −6 cm, and −10 cm) and two distinct positions (central and peripheral) within the experimental setup. In the initial experiment FS1, thermocouples located at a depth of −2 cm experienced complete technical failure, resulting in data collection solely for depths of −6 and −10 cm. During the second experimental condition, FS2, the thermocouples were replaced but the alternative probes at −6 cm encountered complete failure, therefore only the central probe at −2 cm and the peripheral probe at −10 cm collected credible data over the entire experiment length. Despite these technical challenges, the reliable readings obtained from the remaining thermocouples provide valuable insights and facilitate a relative reconstruction of the general heating patterns experienced during the experiment (Fig. 3).

Our experimental design intentionally exposed the sediments and buried bone samples to the furnace during its ramp-up to temperature, ensuring consistency with the prior experiment by Aldeias et al. (2016), which utilized the same fire simulator furnace. This approach also serves as a relative stand-in for the gradual heating process of a combustion feature, where the fire is ignited and progressively reaches its peak temperature.

3. Results

Analysis of the thermocouple data reveals that the temperature ramp-up to the maximum thermal output spanned from 2.5 to 3.3 h, with a slight continued rise thereafter as temperatures were held at 950 °C for an extended duration (Fig. 3). Variations in the slope ramps to attain maximum temperatures at different depths are observed to be influenced by the proximity of each depth to the suspended furnace. After the furnace was powered down, elevated temperatures persisted, gradually dissipating throughout the evening as the sediment was allowed to cool.

The thermocouple data demonstrates that in FS1 bones buried at −6 cm were exposed to temperatures between 175 (peripheral) and 300 (central) °C within 2.5 h of the experiment, corresponding to when the furnace ramped to the maximum temperature of 950 °C (Fig. 3). At −6 cm, this range of approximately 150 °C between the center and edges of the bone cluster continued for the entirety of the experiment, with the maximum recording approximately around 445 °C for the center probe occurring 7.5 h after the furnace was turned on and 3.65 h after the furnace reached 950 °C (Fig. 3). For the same substrate, a mix of gravel and fine sand, at −10 cm depth a temperature range maximally 50 °C between the center and peripheral measurements is seen to start around 4.15 h, with the temperature experienced growing slightly for the duration of the experiment (Fig. 3). The thermocouple probe data suggests that this observed temperature increase was continuing when the probe data collection ended after the duration of the heating period. This data highlights that at −6 and −10 cm the window range of temperatures detected decreases, with the center and peripheral bones at −6 cm experiencing a larger range of temperatures at the shallower depth than bones at −10 cm.

Within FS2, thermocouple data supports the inference that bones buried at −2 cm depth in gravel experienced steady temperatures around 600 °C for at least 4 h, while bones at −10 cm depth in the same

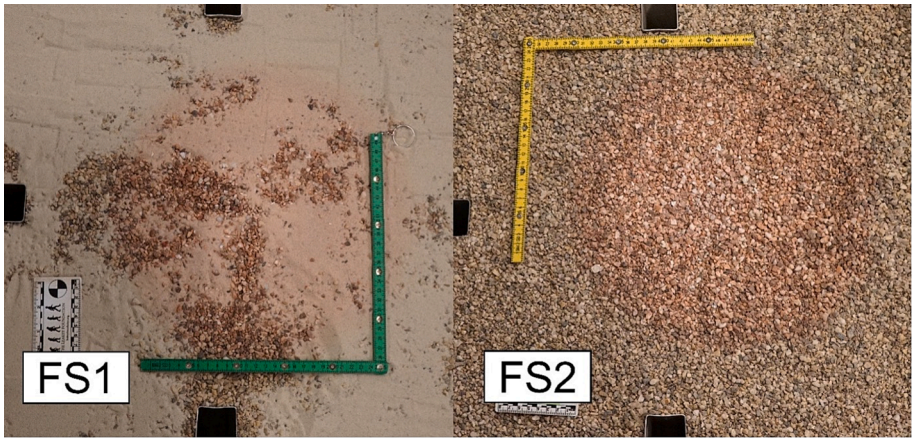

Fig. 2. Rubified substrate of the basin prior to the excavation of buried materials.

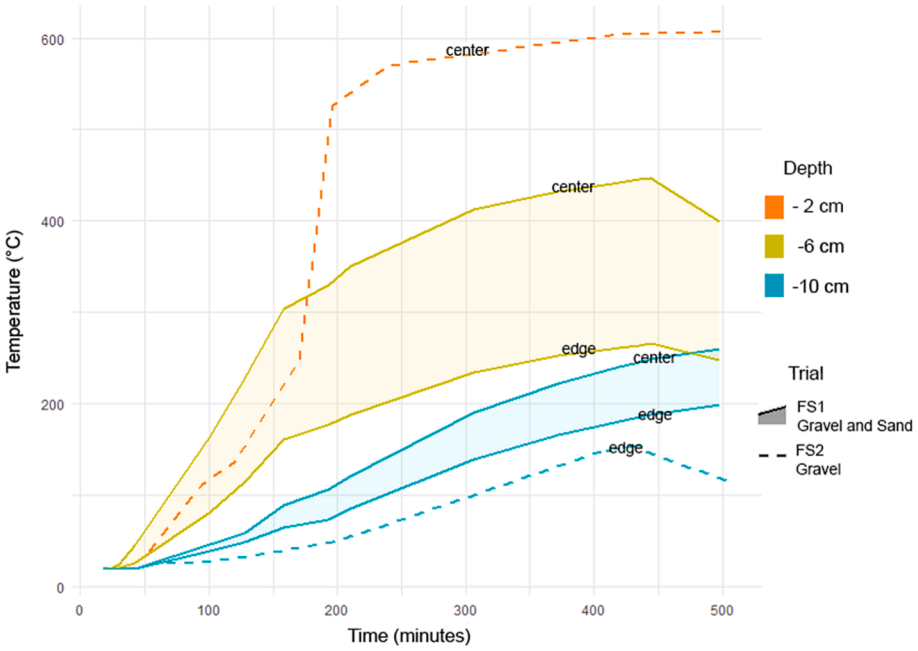

Fig. 3. Compiled thermocouple data from both experimental setups, FS1 and FS2, provides an overview of the thermal variation at tested depths. The furnace apparatus reached maximum emitted temperature of 950 °C over a ramping period of approximately 225 min in each setup. Temperature readings from both peripheral and central thermocouple probes in FS1 offer a range of temperatures from two depths for the duration of the experiment. Data from FS2 presents the credible measurements from the −2 central probe and the −10 cm peripheral probe.

substrate were exposed to temperatures above 100 °C for at least 3.33 h (Fig. 3). Interestingly, in the sole instance where experimental setups can be compared, at −10 cm, the FS2 setup had a lower minimal recorded temperature from the peripheral probe when compared to the peripheral thermocouple of FS1.

3.1. Macroscopic observations

The twelve control 'surface' samples were heated in a Nabertherm muffle furnace at 950 °C for a minimum of 6 h, not including the ramping or cooling period (SI Fig. 23). All fragments were recognized to be uniformly stark white in color (SI Fig. 23). No difference was detected if bones rested on a gravel substrate or gravel and sand. All MF1 and MF2 samples were assigned as Stiner et al. (1995) stage 6, fully calcined (Table 1).

Color variations of bone fragments at the −2 cm depth in both gravel and fine sand (FS1) and gravel (FS2) setups exhibit primarily grey and white colorations but with some detected tans and browns, notably seen in the peripheral bones and interpreted to be signs of depigmented but not calcined bones (Figs. 4, 5). In FS1, bones P_a, N_a, and N_b, would be considered partially calcined and a Stiner et al. (1995) Stage 5 based on visual traits alone, whereas the remaining samples would be considered fully calcined and a Stage 6 (Table 1; Fig. 4; SI Fig. 24). In FS2, peripheral samples M_a and R_a were observed to be a Stiner et al. (1995) Stage 5, while all central samples were assigned to Stage 6, fully calcined (Table 1; Fig. 4: SI Fig. 24).

Samples from both experimental setups at −6 cm depth exhibit a range of colors, including shades of brown, black, tan, and light and dark greys (Figs. 4, 5). For FS1, the darker coloration of M_a, R_a, and O_b may indicate that these bones may have been offset slightly under the furnace during sediment infill, resulting in reduced heat exposure compared to neighboring samples, despite R_a and O_b being positioned more centrally. In both FS1 and FS2, several bones at – 6 cm depth were preliminarily classified using the Stiner et al. (1995) stages 3, 4, 5, and 6, with some flagged for potential depigmentation in muted beige coloration without the surface textures that support indications of calcination (macroscopic cues that are also seen to accomapny prolonged in prior experiments; Gallo et al., 2023; Table 1). Notably, in FS2, a peripheral sample, M_b, was observed with darkened, greasy gravel adhering to the underside of the fragment (Fig. 4; SI Fig. 24).

At −10 cm depth, bones were categorized as Stiner et al. (1995) stages 1, 2, and 3, and exhibited colors ranging from light and dark brown to black (Figs. 4-5). In FS2, two peripheral samples again showed darkened, greasy gravel adherence, but at this depth, the soot covered sediment adhered to all sides of the fragments (SI Figs. 18–22, 24).

This presence of "greasy char" seen adhereing to both the bones and gravel warrants further investigation. One hypothesis is that the darkened, soot-like appearance might result from volatile organic compounds released during bone burning. These gasses could condense onto surrounding gravel, particularly under conditions of lower temperatures and/or (semi-)reducing environments. This aligns with observations of greasy residues in fires with insufficient oxygen or incomplete combustion (Hoare et al., 2023; Krap 2022).

Alternatively, the greasy and soot-like appearance could represent a tar-like byproduct formed from partially combusted organic materials within the bone, especially at peripheral or less-heated zones where combustion may not have been complete. However, we cannot confidently conclude the precise mechanism responsible for this phenomenon at this stage. Future experiments designed to replicate and expand on these analyze these conditions more systematically could expect such formations at −10 cm depths and investigate the presence of these residues in relation to semi-reducing environments.

3.2. Burning codes based on visual observations

Utilizing first only macroscopic visual indicators, burning stages were blindly assigned following a modified Stiner et al. (1995) scale, with extra stages provided to account for the depigmentation observed in a concurrent experiment (Gallo et al., 2023) in modern bone (Tables 1-2).

3.3. FTIR-ATR

Infrared spectroscopy (FTIR-ATR) was employed here to provide

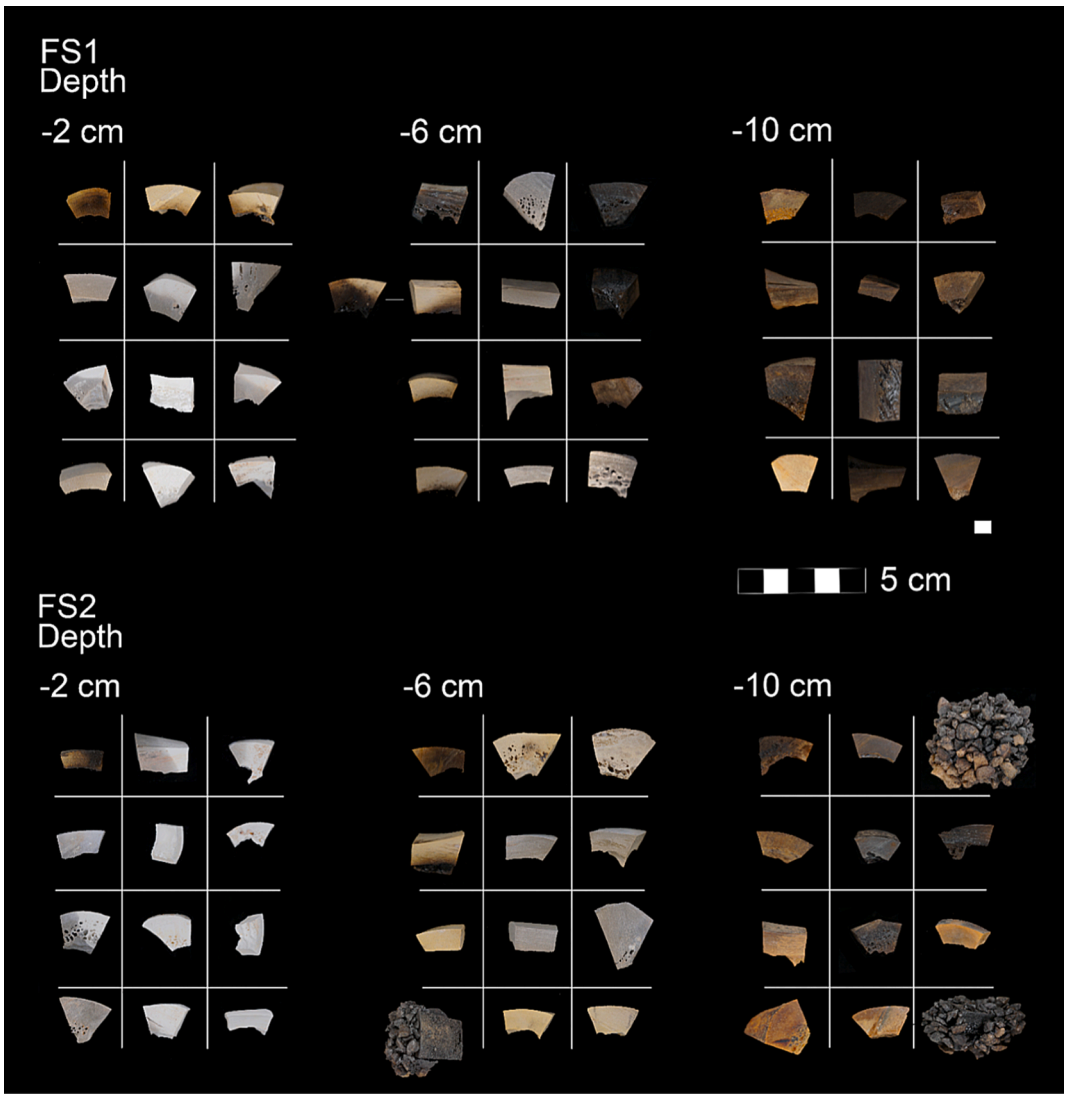

Fig. 4. Experimental setups FS1 and FS2 bone post-heating, arranged by depth in plane view. View here is consistent between depths and experimental conditions, with the top and bottom row of each set representing the peripheral samples of the burial arrangement. Bone fragments are photographed from the side in their post-excavation state. This includes dark, sooty, and greasy deposits which adhered to a few samples.

semi-quantitative insights into the thermal effects on buried bone. Spectra were evaluated for key indicators of heat alteration, including the extent of organic and carbonate loss, the presence of OH vibrational signals, and the formation of cyanamide (which can reflect thermal changes under reduction atmospheres). Additionally, this data was used to monitor the growth and transformation of bioapatite through indicators of increasing crystallinity, as well as the formation of phosphate peaks related to heat-induced changes to assess whether the bones exhibit characteristics of calcination.

All samples subjected to heat as a controlled 'surface' set in the Nabertherm muffle furnace have spectra characteristic of calcined bone (SI Fig. 3, 18). This includes a full elimination of organics and a barely present doublet absorption CO_3^{2-} v3 functional group, indicating the depletion of structural (type B) lattice carbonates (Fig. 6). These small peaks typically persist until temperatures of 1000 °C in fresh samples burned in air (Fig. 6; Gallo et al., 2021). Two peaks dependent on high-heat transformation linked to OH moieties are clearly apparent here (Mamede et al., 2018a, 2018b; Marques et al., 2016; Snoeck et al., 2014). These peaks are reported to become visible after temperature exposure of 600 °C and include the OH librational mode, a shoulder also referred to as the PHT on the side of the PO_4^{3-} v4 (605 cm^{-1} band, measured at 630 cm^{-1}), and the OH stretching mode at approximately 3572 cm^{-1} (Fig. 6; SI Fig. 25). The presence of these peaks indicates these samples were burned in the presence of air, supported by the absence of aromates and no peaks at 700 and 2000 cm^{-1} which are reported in experimental reduction atmospheres and linked to cyanamide (Mamede et al., 2018; Reidsma et al., 2016; for full review see Marques et al., 2021).

Further evidence supporting this inference of exposure to high heat and structural and chemical transformation with calcination is the sharp shoulder separating from the PO_4^{3-} v3 peak at ~ 1090 cm^{-1}, a measure reported to be the presence of francolite, a carbonate florapatite mineral produced by the changing chemistry and structure of the bone material with heat exposure (Mamede et al., 2018a; Patonai et al., 2013). This shoulder has been produced in experimental conditions above temperatures of 700 °C in bone exposed to air burned for 10 min, 30 min, 90 min, and for 9 h (Gallo et al., 2021). It is also seen accompanying calcined samples at 550 °C for 9 h (Gallo et al., 2023). The two peak maxima of the general band assignment for the phosphate antisymetric mode PO_4^{3-} v4 peak areas are also separated in all muffle furnace samples by a deep trough, indicative of a higher order of crystallinity than fresh bone (Fig. 16).

Focusing now on the experiments with the fire simulator heat source, in FS1, a substrate of gravel and fine sand, at a depth of −2 cm four

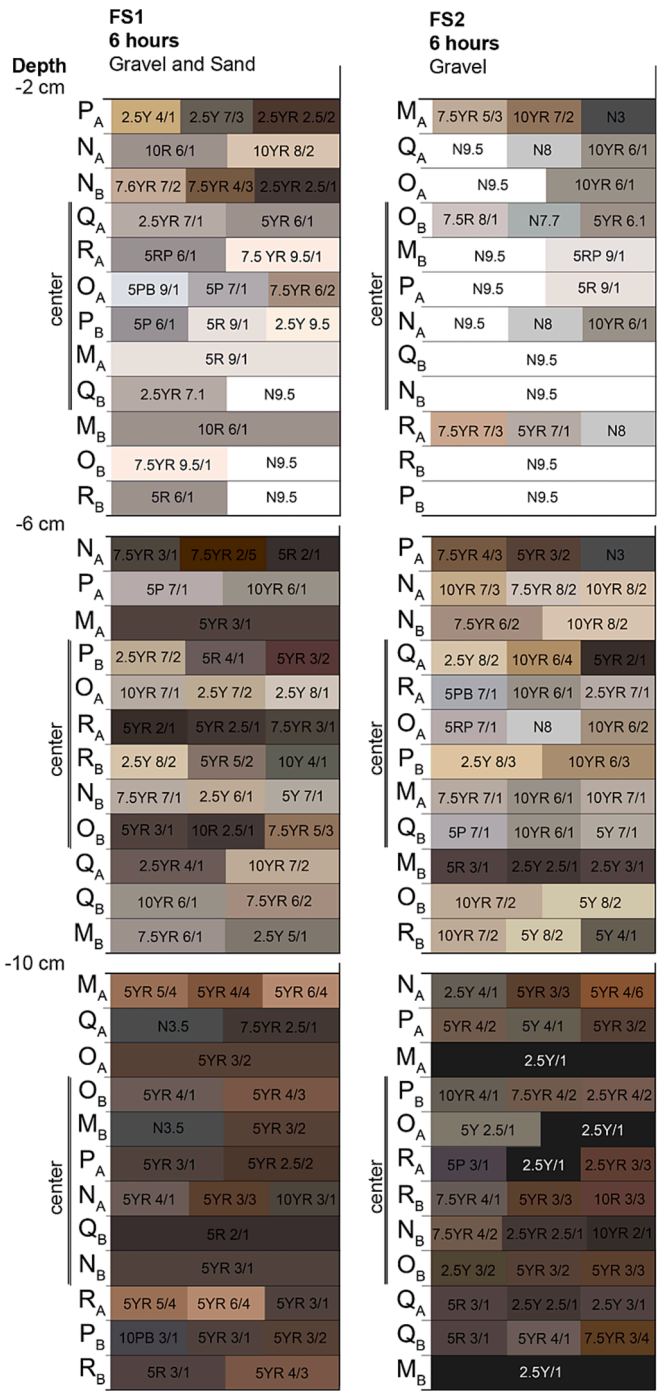

Fig. 5. Munsell color code results taken on bone fragments post-heating and excavation for each experimental condition at −2, −6, and −10 cm depths. A Color Gun RM2000 CAPSURE Color Matching tool was used to obtain color codes, and multiple are presented for when more than one color was detected on the fragment. Bones with 'central' placement in the cluster in the middle of the thermal footprint of the furnace are denoted with a double vertical line. † 6 h indicates the duration samples were held at temperature excluding the heating ramp and cooling period.

samples (N_a, N_b, P_a, Q_a) are not calcined (Fig. 7). Three of these are peripheral samples, closest to the top edge of the furnace footprint (Figs. 4, 7; SI Fig. 24). Two samples, M_b and O_a, are classified here as experiencing elevated temperatures close to but under ~600 °C, as they have spectral signatures of being impacted by high temperatures but are not calcined. Both M_b and O_a do not have organic material preserved and have a small start of OH stretching vibration at ~ 3572 cm^{-1}, supporting an inference of burning in oxygen atmospheres (SI Fig. 25). These samples do have present lattice carbonates and do not have prominent high-temperature shoulders at ~ 1090 cm $^{-1}$ or 630 $^{-1}$, indicating they have not experienced the thermal energy necessary to become fully structurally and chemically calcined (Fig. 7). The spectra of samples N_a, N_b, P_a, and Q_a resemble spectra of bones burnt in air to ~300–500 °C based on observations regarding the Amide I and II functional group area and inferred carbonate content (Fig. 7; Gallo et al., 2021; 2023). Calcined samples M_a, O_b, P_b, Q_b, R_a, and R_b exhibit spectra similar to those of the surface 'control' muffle furnace setups, including large splitting on the PO_4^{3-} v4, both the high temperature PHT and ~ 1090 cm^{-1} shoulders, and a clear sharp OH stretching vibration (Fig. 7).

In only gravel substrates in FS2, three samples (M_a and R_a, both peripheral, and O_b, central) did not calcine at −2 cm under the surface (Fig. 7). Of these three, the central sample O_b does not have any organic components remaining as observed from the FTIR-ATR spectra (Fig. 7). O_b also does show suggestions of the start of high temperature alteration however through suggestions of ~ 630 cm^{-1} and ~ 1090 cm^{-1} shoulders off of the v4 and v3 phosphate peaks: an example of a sample beginning to have the structural and chemical transformations that accompany calcination (Fig. 7). This sample is therefore thought to have experienced slightly elevated temperatures compared to the other non-calcined bones at the same depth. Of all FS2 −2 cm bones, only M_a does not have a OH stretching vibration peak visible at approximately 3572 cm^{-1}, prompting questions for the timing of the presence and intensity of this band within samples that do not yet have other indications of increased lattice organization and other measurable alterations to the mineral phase (SI Fig. 25). The observations of an OH signal in other samples does support that bones had access to oxygen in FS2 as well as FS1 at −2 cm. Remaining samples M_b, N_a, N_b, O_a, P_a, P_b, Q_a, Q_b, and R_b were identified as calcined based on the absence of organics, the minimal carbonate doublet at CO_3^{2-} v3, the OH stretching at ~ 3572 $cm^{-1,}$ the clear high-temperature shoulders at ~ 1090 cm^{-1} and ~ 630 cm^{-1} (OH libration, the PHT shoulder; Fig. 7; SI Fig. 25).

At a depth of −6 cm in a substrate of mixed gravel and fine sand (FS1), one peripheral sample, P_a, can be considered as calcined (Fig. 8). P_a has had all organic residue removed, has very little present lattice carbonate, and has a sharp OH stretching peak at ~ 3572 cm^{-1}. Distinguishing this sample further from the eleven other samples buried at −6 cm is the slight but detectable OH libration as a shoulder on the PO_4^{3-} v4 peak area (PHT) and the ~ 1090 cm-1 nominal shoulder on the PO_4^{3-} v3 peak (Fig. 8). Again, this OH signal does indicate bones were thermally altered primarily in the presence of oxygen in a mixture of gravel and sand here at −6 cm (SI Fig. 25). Other samples from this depth exhibit greater peaks related to the presence of Amide I and II, and carbonates seen to be impacted to a similar degree as bones heated in air at controlled temperatures of ~300–500 °C (Fig. 8; Gallo et al., 2021).

Only one sample in gravel (FS2) at −6 cm depth is also calcined. This fragment, Q_b, is from a central position within the cluster and has more pronounced evidence of thermal alteration than the calcined counterpart at FS1 −6 cm (Fig. 8). This is observed through stronger and sharper peaks related to high-heat transformation of the bioapatite mineral and more decreased proportion of carbonates (Fig. 8). Two samples have suggestions of the shoulders which will become more pronounced with calcination on the phosphate peaks as well as having no organic content and minimal remaining lattice carbonates: O_a and R_a. These samples are interpreted as having experienced temperatures approaching calcination, exceeding those of other non-calcined bones at the same depth (Fig. 8). Samples M_a, O_b, and Q_b have an observable peak at ~ 3572 cm-, despite only O_b exhibiting at PHT shoulder (Fig. 8; SI Fig. 25). This OH signal and the lack of peaks at 2000 and 700 cm $^{-1}$ also suggest that these bones were also burned in an mostly oxygen atmosphere.

No bones are calcined at −10 cm in either a mixture of gravel and sand (FS1) or only gravel (FS2; Fig. 9). From the spectra in both setups, it can be confidently estimated that temperature exposure at this depth was limited to ~100–300 °C due to the amount of water, organic, and

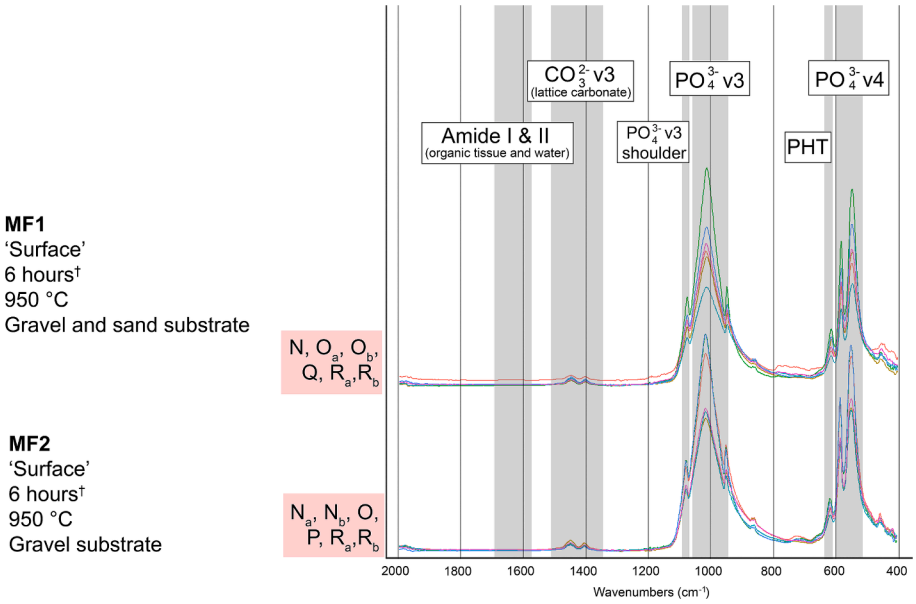

Fig. 6. FTIR-ATR spectra of both muffle furnace runs (~400–2000 cm^{-1}) for control 'surface' samples. The distinct colors of the spectra represent individual samples analyzed in this study. † The 6-hour duration reflects the time samples were maintained at the target temperature, not including the heating and cooling phases.

lattice carbonate content. There are also minimal transformations to the bioapatite mineral, indicating limited thermal alteration at this depth. The minimal structural and chemical changes in the bone samples caused by low heat exposure prevent definitive conclusions about the burning atmosphere. Spectroscopic markers allowing for a more confident assessment of reduction atmospheres only become apparent at higher temperatures (SI Fig. 25).

3.4. FTIR equations

All ratios calculated for this study support the primary observations on the FTIR-ATR spectra. The CO/P ratio which evaluates the organic components present demonstrates very low values for the controlled muffle furnace 'surface' samples as well as at −2 cm depths in both substrates (Fig. 10). At −6 cm depths a greater range is seen, noting the differences between bones tested from different positions in the arrangement under the furnace footprint (Fig. 10). At −10 cm values are relatively large, separating almost entirely from the −6 cm samples, supporting the inference that bones at this depth only started the decomposition stage of burning and for several bones in peripheral positions are only partially burnt (Fig. 10).

The C/P ratio assesses the relative amount of lattice carbonates present in a sample, a metric that is expected to experience decreases starting around 400 °C, be present only as a minimal doublet from approximately 700–900 °C, and disappear entirely at 1000 °C (Gallo et al., 2021). C/P ratios in this study follow the visual observations closely, with a step-wise pattern noted for each depth tested (Fig. 11). Samples burned in the muffle furnace have the lowest ratio, with the −2, −6, and −10 cm depths each with significantly different means increasing in value as a function of depth (Fig. 11).

While peaks were visible for many spectra at 3572 cm^{-1}, the OH/P ratio utilizing the ~ 3572 cm^{-1} peak height and the 605 cm^{-1} peak height as a part of the PO_4^{3-} v4 band assignment was less successful in providing information regarding temperature estimation and impact of thermal exposure (Fig. 12). Values are reported here to contribute to the development of this ratio for research regarding the thermal alteration of bone material (Mamede et al., 2018b). The use of the librational mode of OH, the peak at 630 cm^{-1}, was a more useful indicator of calcination across all depths (Fig. 13). PHT ratio values > 1 tracked closely with all calcined samples except for FS1 −6 cm sample P$_a$, which still had a larger value than all non-calcined samples measured. Interestingly, the −2 cm depth had the largest ratio values despite the inference that the 'surface' muffle furnace samples experienced more direct heat and thermal energy (Fig. 13). These values from this experiment testing 6-hour durations at 950 °C (in addition to the ramping and cooling temperatures) are also lower than values seen in from a muffle furnace with ten minutes at 750 °C (Gallo et al., 2023). The values seen in this experiment are closer to PHT values testing a duration of 9 h at 750 °C, prompting questions for future research regarding the utilization of OH signals for the consideration of high temperature and long duration thermal alteration (Gallo et al., 2023).

The splitting factor, a ratio representing the relative degree of crystallinity based on the size and order of the bioapatite crystals, demonstrates a pattern of decreasing values between the −2, −6, and −10 cm depths (Fig. 14). All samples designated as calcined here have SF values 4.2 or greater except for one bone, FS1 −2 O$_a$, which has an SF value of 4.3 and was one of the samples designated as nearly calcined. The lowest SF of calcined samples is from the muffle furnace control setup on only gravel substrate (MF2 N$_b$) with a value of 4.285. This sample was one selected for complementary XRD analyses to see if the SF value was low due to extensive alteration from the coalescence of the mineral crystals, resulting in a negative relationship between the SF ratio and temperature intensity experienced.

To assess the effect of substrate type (the mix of gravel and sand, FS1, or only gravel, FS2) and depth (surface, −2, −6, and −10 cm) on the degree of heat exposure as measured through the SF ratio, we first evaluated normality by visualizing the data with histograms. A Shapiro-Wilk test provided evidence to reject the null hypothesis of normality, indicating the data was distributed non-normally. Therefore, we fit a linear regression model on the natural logarithm of SF.

Ordinary least-squares regression was used to model the natural logarithm of the SF response variable as a function of substrate (FS1, FS2) and depth predictor variables (Table 3; Fig. 15; SI 'Model Results'). The natural logarithm of SF was chosen to satisfy residual normality assumptions of OLS regression. The overall model explains ~ 34 % of the variance in log SF (R2 = 0.34). The exponentiated intercept (1.55, 95 % CI = 1.497, 1.611) is the geometric mean of log SF for the baseline category (FS2) when depth equals 0 (e1.55 = ~4.73; Fig. 15, SI) The estimated slope coefficient (0.03, 95 % CI = 0.022, 0.037) is the projected change in log SF for a one-unit change in depth. The

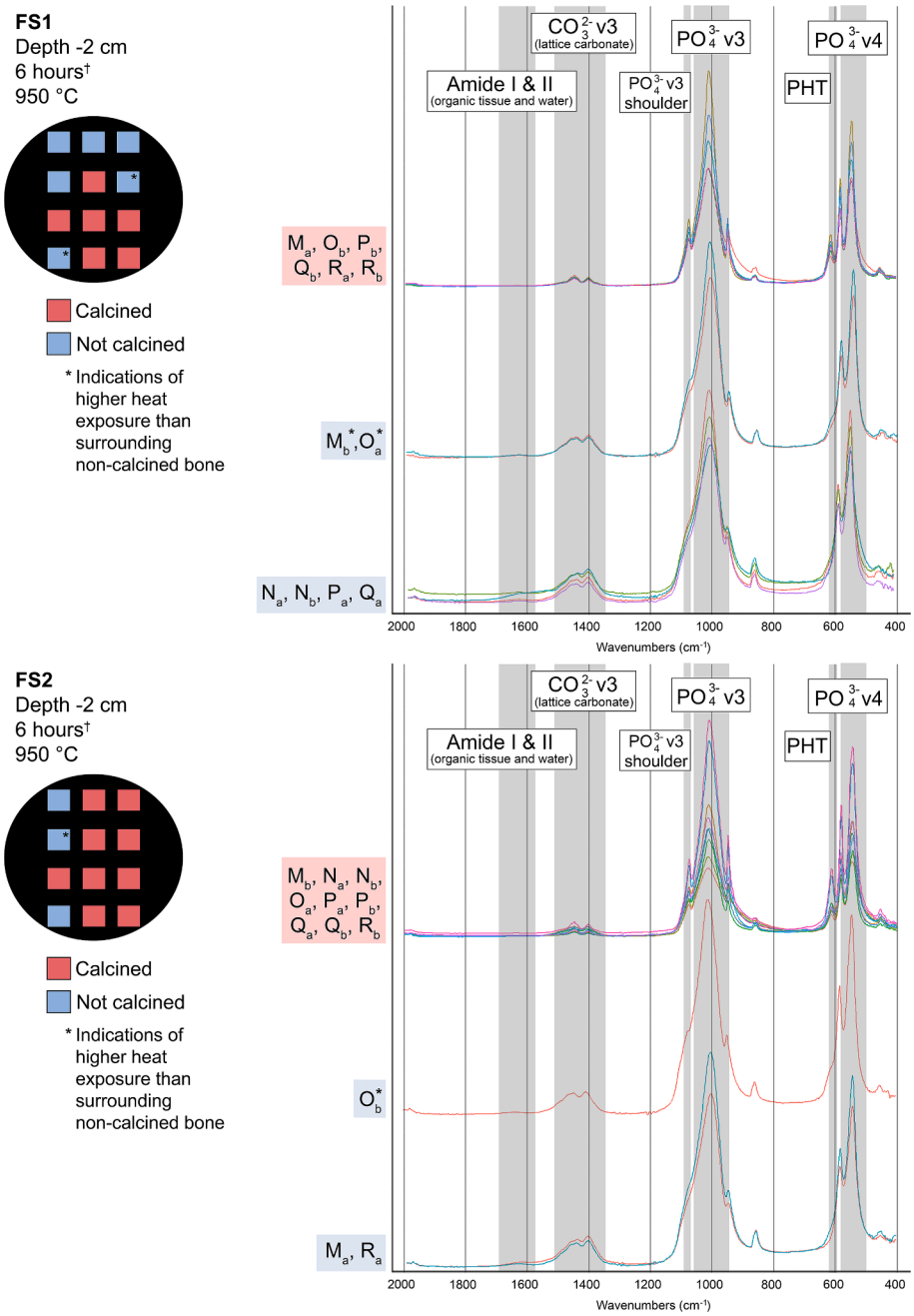

Fig. 7. FTIR-ATR spectra of all bones from FS1 and FS2 at −2 cm depth (~400–2200 cm^{-1}). Spectra have been separated into groups based on the extent of heat modification for ease of visualization. Samples identified after analyses as calcined are highlighted by a red box. Each spectrum is assigned a unique color to indicate a specific sample.† 6 h indicates the period samples were held at temperature, excluding the time required for heating up and cooling down.

exponentiated coefficient for substrate (−0.06, 95 % CI = −0.109, −0.002) is the ratio of geometric means of log SF for FS1 to FS2 (e-0.06 = ~0.95). Therefore, the linear model describes a positive relationship between the logarithm of the SF ratio values and depth with a small but meaningful negative effect seen in FS1, a substrate of both gravel and fine sand.

In summary, increasing depths are associated with a decreased log SF, an expected result given the lower SF values are a direct consequence of lower temperatures at deeper depths. Higher ratio values are associated with the inferences of higher crystallinity, and higher crystallinity is seen in samples which experienced a greater amount of heat exposure. This relationship is further mediated by substrate type, with small but detectable differences implying that bones buried in the gravel only substrate (FS2) experienced a higher degree of heat proportional to the depth of each tested bone sample. Additional research with larger sample sizes and different substrate granulometries can contribute to improving this model and test the hypothesis of substrate effect, as the accuracy and usefulness of this model is limited by the scope of the experimental sample size. Despite this, the inference that bones in FS2 experienced greater heat can also be substantiated by the greater number of calcined samples and samples that experienced temperatures approaching calcination at the −2 cm and −6 cm depth, as well as potentially greater heat retention at −10 cm which may be responsible for the conditions favorable for producing the greasy, soot-like substance which adhered to several peripheral samples.

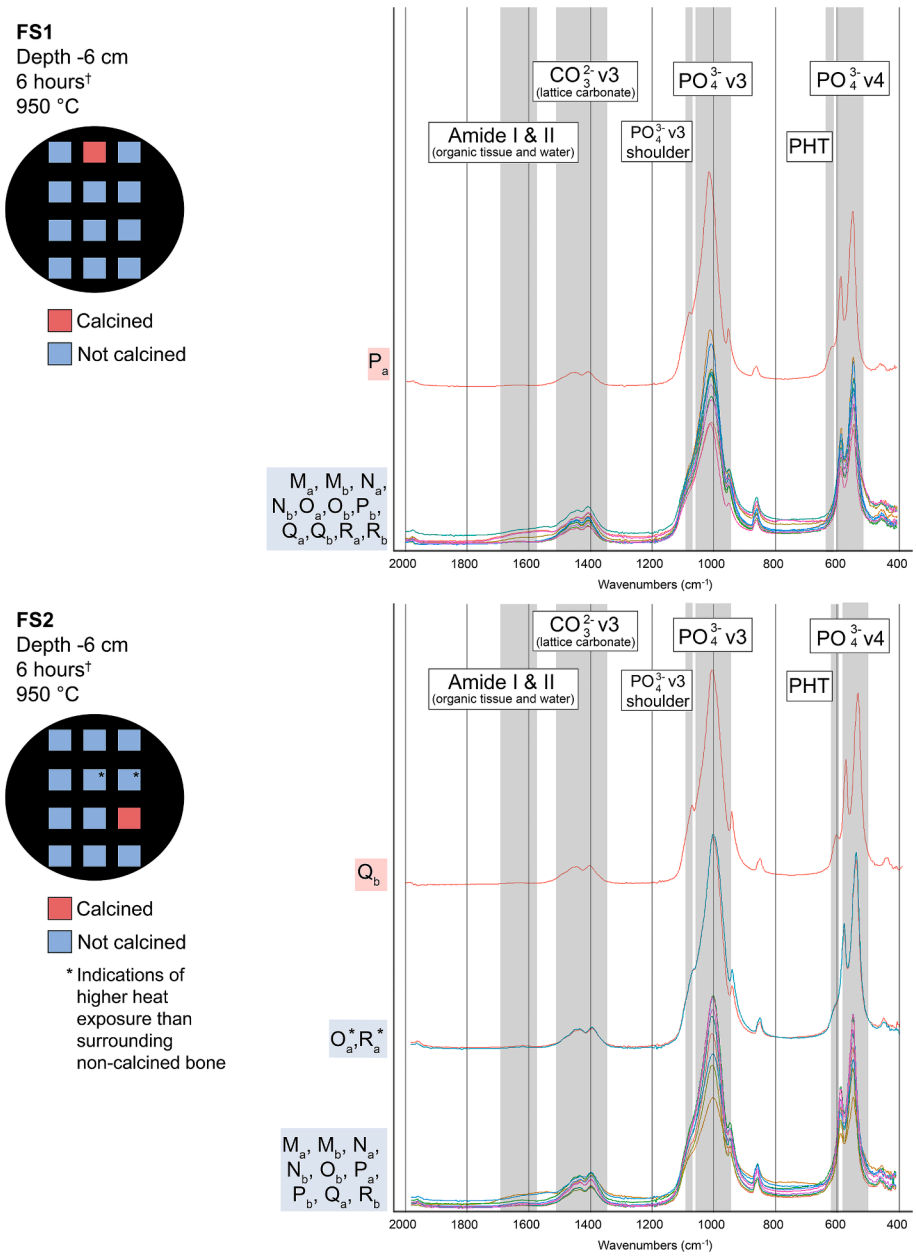

Fig. 8. FTIR-ATR spectra of all bones from FS1 and FS2 at −6 cm depth (~400–2200 cm^{-1}). Sample Pa from FS1 and Q_b from FS2 are calcined, and therefore identified in red and separated for better visualization. The distinct colors of the spectra represent the different spectra at – 6 cm depth. † The 6-hour period refers specifically to the time samples were kept at the target temperature, excluding the heating ramp and cooling stages.

3.5. XRD

Five bone samples from the experimental setup set on gravel (MF2) and buried in gravel substrates (FS2) were selected for complementary XRD measures of average crystallite size and compared to a referential dataset of bones burned in air at different durations and temperatures (Gallo et al., 2021, 2023). From MF2, bone N_b was chosen due to the lowest SF value (4.258) observed of all calcined samples. Representing bones from the −2 cm depth of FS2, bone R_b was tested to represent one of the highest SF values (5.675) produced in all experimental setups. Finally, also from FS2, bone O_b was selected due to the grey coloration, and the status as nearly calcined without clearly pronounced spectral qualities representing calcination. Two bones were also selected from the −6 cm depth of FS2. Bone R_a represents a grey and white bone fragment also designated as experiencing higher temperatures just under calcination. Bone Q_a was picked as it is a very clear example of the assigned modified Stiner et al. (1995) stage of 3D, depigmentation with presence of carbonization.

As measures of relative crystallinity from the FTIR-ATR spectra can be nonreliable at high temperatures, the average crystallite size determined using Rietveld refinement provides an independent measure of crystallite growth. Results indicate that bone FS2 R_b from −2 cm depth has the largest average crystallite size, larger than bones burnt at 900–1000 °C in air for 30 min (Fig. 16; Gallo et al, 2021). Bone N^b from MF2 also has a large average crystallite size, in line with values expected from thermal alteration for 30 min between 900 and 1000 °C (Fig. 16). This low SF value is therefore in line with expectations of SF values declining with high temperature exposure.

Bones O_b (− 2 cm depth) and R_a (−6 cm depth) have very similar average crystallite size values, with R_a having a slightly larger average size when compared to O_b despite being buried at a deeper depth (Fig. 16). Both of these values are below a threshold seen to accompany

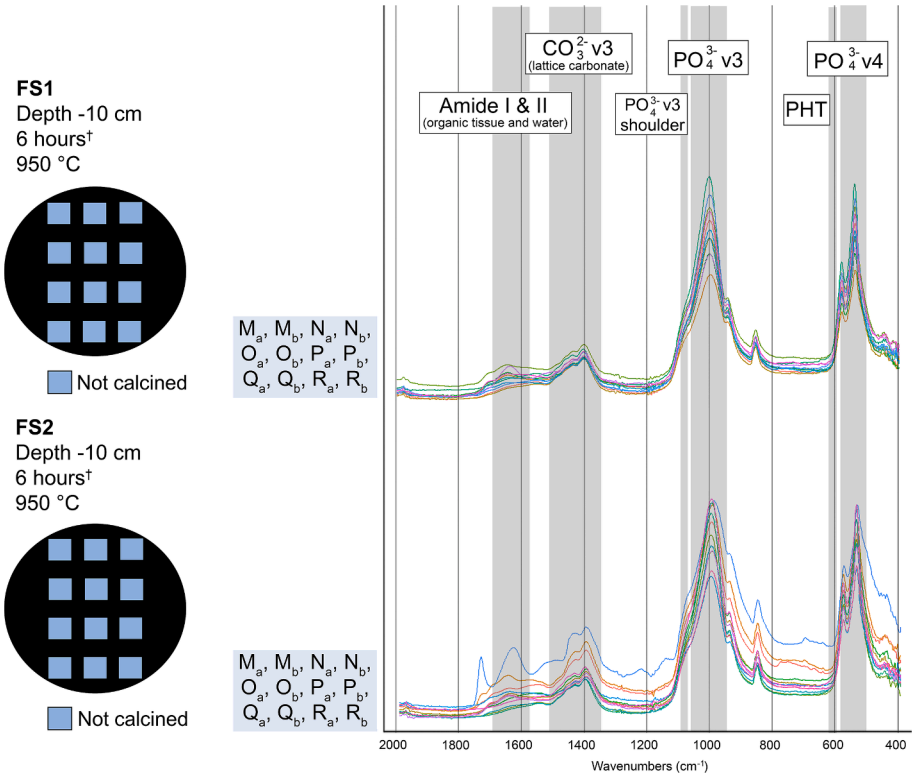

Fig. 9. FTIR-ATR spectra of all bones from FS1 and FS2 at −10 cm depth (~400–2200 cm^{-1}). Interference from the gravel substrate adhering to the sample surface of sample Ma in FS2 is responsible for the abnormal spectral signature. The variation in spectral colors reflects the different samples. † 6 h held at temperature excludes the time bringing the furnace to temperature or the cooling period.

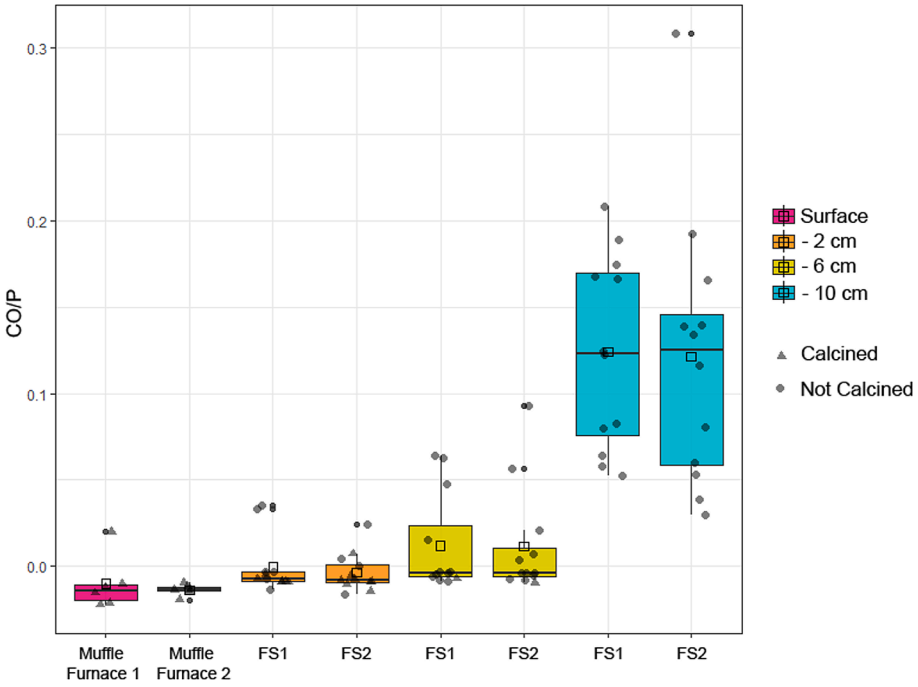

Fig. 10. CO/P ratio across all experimental conditions and depths for evaluation of organic components subsequent to heating. Muffle furnace 1 and Fire Simulator setup 1 (FS1) both represent substrates of gravel and fine sand, while muffle furnace 2 and Fire Simulator setup 2 (FS2) consisted of only gravel sediments. Samples determined to be calcined after analysis are here identified by a triangle icon.

calcination in the experimental referential dataset (35 nm), supporting the inference that they are not yet fully calcined despite having slight spectral indications of undergoing transformations at high temperatures. Bone Q_a has the lowest value in terms of average crystallite size (Fig. 16).

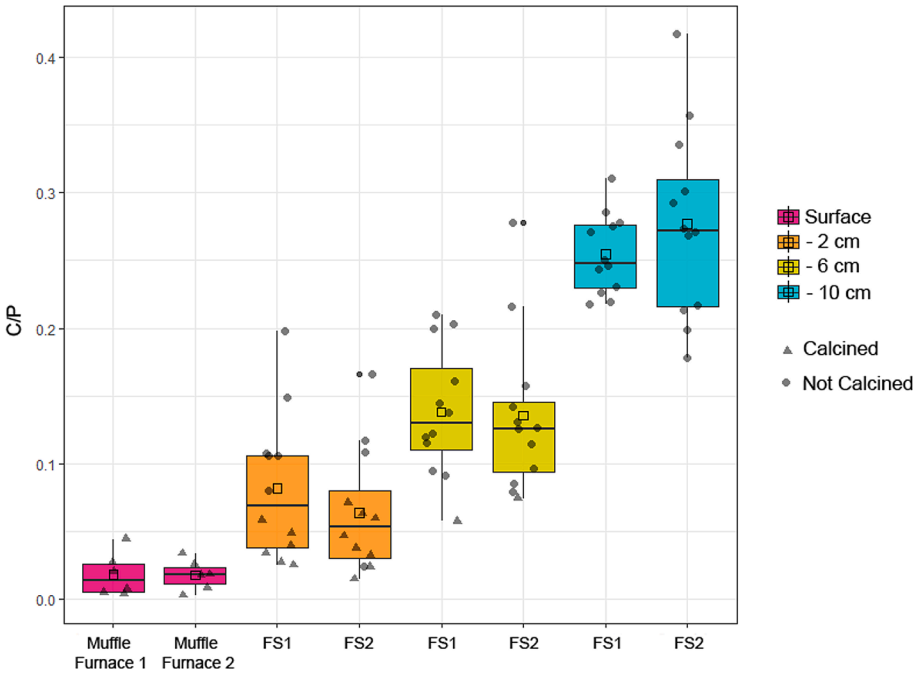

Fig. 11. C/P ratio across all experimental conditions and depths. Muffle furnace 1 and Fire Simulator setup 1 (FS1) both represent substrates of gravel and fine sand, while muffle furnace 2 and Fire Simulator setup 2 (FS2) consisted of only gravel sediments. Samples determined to be calcined after analysis are here identified by a triangle icon.

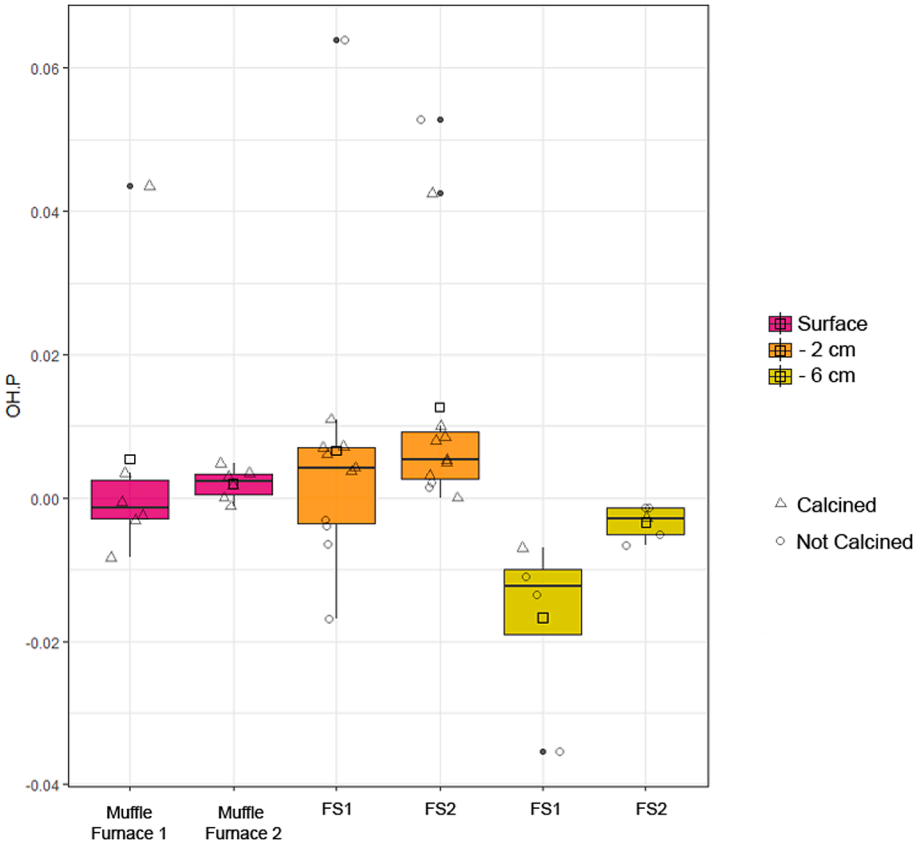

Fig. 12. OH/P ratio across samples which exhibited an OH– signal at 3572 cm^{-1}. Muffle furnace 1 and Fire Simulator setup 1 (FS1) both represent substrates of gravel and fine sand, while muffle furnace 2 and Fire Simulator setup 2 (FS2) consisted of only gravel sediments. Samples determined to be calcined after analysis are here identified by a triangle icon.

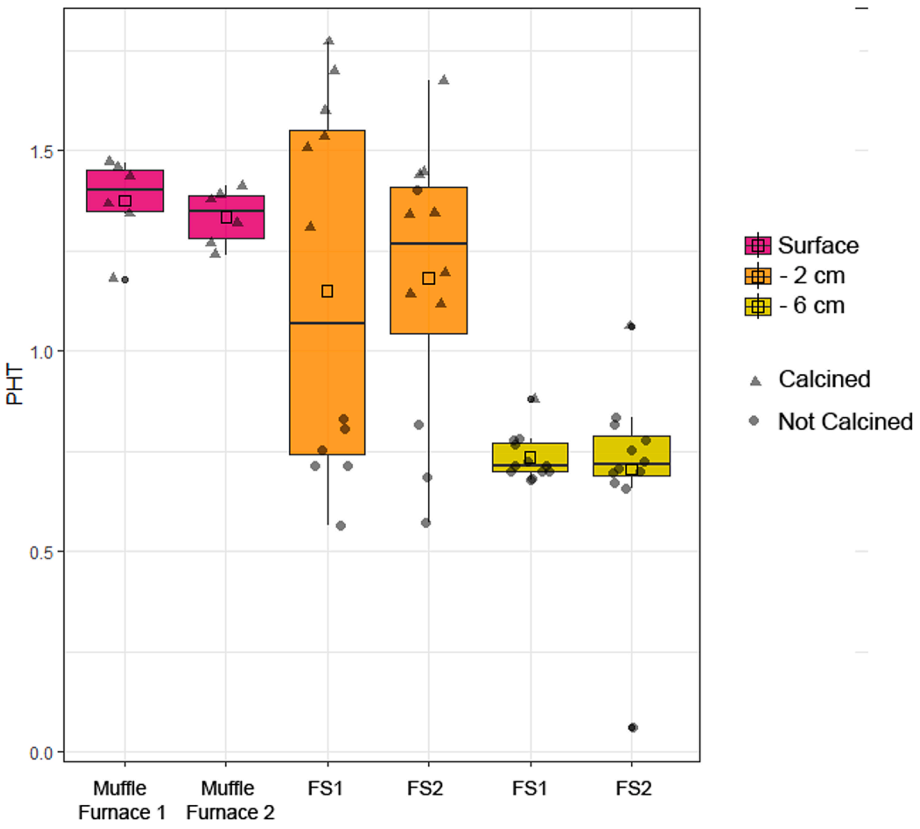

Fig. 13. PHT ratio across samples which had a peak present at ~ 630 cm^{-1}. Muffle furnace 1 and Fire Simulator setup 1 (FS1) both represent substrates of gravel and fine sand, while muffle furnace 2 and Fire Simulator setup 2 (FS2) consisted of only gravel sediments. Samples determined to be calcined after analysis are here identified by a triangle icon.

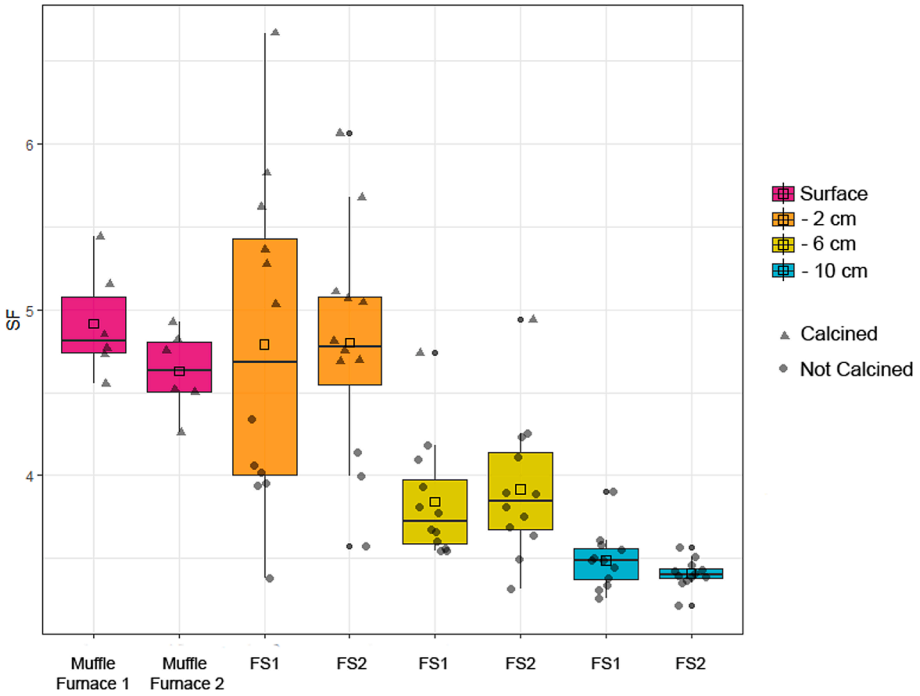

Fig. 14. SF ratio for all samples. Muffle furnace 1 and Fire Simulator setup 1 (FS1) both represent substrates of gravel and fine sand, while muffle furnace 2 and Fire Simulator setup 2 (FS2) consisted of only gravel sediments. Samples determined to be calcined after analysis are here identified by a triangle icon.

Table 3
The estimated effect of substrate and depth on log splitting factor.

	Estimate	Std. Error	*t*	*p*
Intercept	1.55	0.029	54.22	< 0.001
Gravel and fine Sand (FS1)	−0.06	0.027	−2.04	0.0433
Depth	0.03	0.004	7.77	< 0.001

3.6. Revisions to the burning stage designations

Based on the results of the spectroscopic analyses, the initial burning stage designations following a modified Stiner et al. (1995) scale were revisited (Table 2). Any discrepancies between the determinations of calcination and visual cues of Stiner stages 4–6, partial presence of calcination to fully calcined, are highlighted here (Table 2). In twelve instances, at the −2 and −6 cm depths of both substrates, observations of pale grey represented bones that were not calcined and were therefore incorrectly identified (Table 2). Bones were correctly recognized as depigmented and not calcined when their coloration was more similar to pale tans and browns (Table 2). This result notably calls attention to the dangers of using color identification to infer high temperature alteration without spectroscopic validation and supports prior research finding that bone color is tied closely to the presence of carbonized and charred organic remains in bone which can dissipate with long durations at lower temperatures and is not inherently an indication of calcination or any specific temperature value (Gallo et al., 2023).

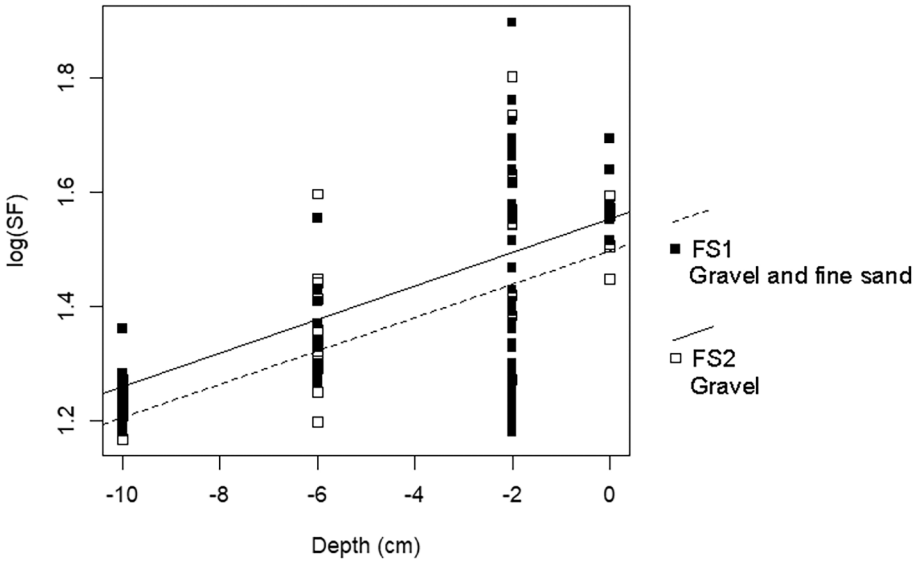

Fig. 15. Relationship between burial depth and Splitting Factor (SF) by substrate type. Each data point represents the logarithm of SF measured at different depths, categorized by substrate type (gravel and fine sand, FS1, and only gravel, FS2). The dashed line represents the trend for the mixed gravel and fine sand substrate, while the solid line represents the trend for only gravel substrate, log(SF) = 0.03 depth – 0.06 substrate + 1.55. Variation in SF values at each depth are expected, as bones experienced different degrees of heat exposure based on their arrangement under the Fire Simulator furnace, so the predictive value of this model is limited.

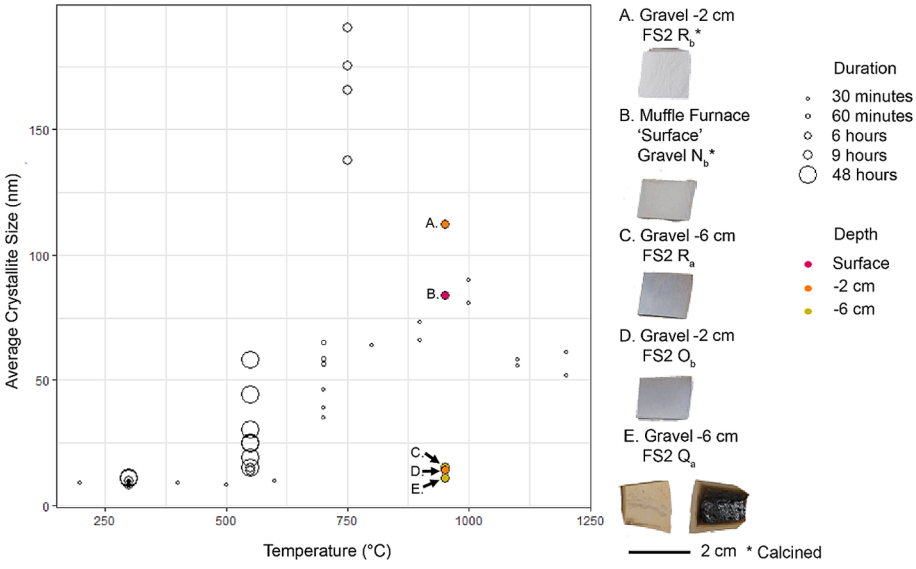

Fig. 16. Synthesis of average crystallite sizes (nm) from several referential databases on bone burned in air (Gallo et al., 2021; 2023). Samples from this experiment, burned at 950 °C for 6 h, are identified with A-E designations and color coded to burial depth. Bone fragment Q_a here shown in two orientations to illustrate the coloration of a depigmented sample with the presence of carbonization.

4. Discussion

Bones offer valuable insights into ancient fire events, providing information on relative temperature, atmosphere, and duration. This study helps to establish expectations for interpreting archaeological thermally altered bone and highlights the conditions necessary for significant bone alteration to occur under fire events (Fig. 17). The potential for buried materials, like bone, to be affected by surface combustion events does presents a challenge due to the difficulty in determining the stratigraphic relationship between buried materials and the original fire event in archaeological contexts. If buried bone greatly predates the later fire event that altered it, the presence of burned bone alone at a given layer cannot be directly interpreted as fire use during that time or as intentional incorporation within the fire event. The experiment presented here, however, helps estimate the possible impacts of subsurface alteration of bone, which in turn can inform archaeological interpretations. Even in our experimental setup that used high intensity sustained temperature during long durations, most buried bones were not calcined, although calcination did occur in two bones at −6 cm, and some were fully carbonized at −10 cm.

The conditions necessary for significant impact on buried bone—whether carbonization/charring or calcination— require fires with surface temperatures high enough to affect underlying materials. While a temperature at the top range of realism for an unstructured, anthropogenic fire was tested here, further testing of a range of temperatures will help scale the impact more accurately. Aldeias et al. (2016) establishes that long duration periods, approximately 2–3 h, are essential for heat penetration into the substrate. Data available regarding natural grass wildfires indicate burning lengths under this duration, and with predominate temperatures less than or around 300 °C (for summary, see Stahlschmidt et al., 2023), suggesting that such fires would not leave signatures on buried fauna in the substrate. However, dung, tree stumps, and peat natural fires have been observed to reach higher temperatures which can mimic anthropogenic fire conditions (Buenger, 2003; Gowlett et al. 2017; Pyne et al., 1996; Whelan, 1995).

A broader range of natural wildfire conditions must be tested to further explore the relationship between combustible materials in different biomes, duration times, and temperatures reached. This presents challenges for zooarchaeological research using thermally altered bone to document anthropogenic fire, as burned bone beneath a combustion feature may not have been intentionally included in the fire but can be recognized as such. Cautious interpretations of burned fauna are therefore recommended, given the presence of carbonized bone observed at −10 cm and two examples of calcined samples recovered at −6 cm in this study, one in each substrate condition.

We emphasize in archaeological contexts the need to test and document the post-depositional processes; the microcontextual approach (Goldberg et al., 2017; Mallol and Mentzer, 2017; Stahlschmidt et al., 2015). The inclusion of this information can assist with making more confident assumptions about how faunal material is related to archaeological combustion features. Nonetheless, data from thermally altered bone regarding the temperature of alteration and burning atmosphere remain pertinent for understanding the conditions under which thermally altered bone were exposed to, even if unintentionally. It is further reassuring for research testing burned fauna are the observations that lateral heat dispersion is limited both on the surface and beneath features, documented both in Aldeias et al. (2016) and through the patterns of burning intensity noted in this study. Accordingly, we suggest only bones directly under combustion features are vulnerable to considerable incidental heating.

4.1. *Predicted impact of different variable conditions on the thermal alteration of buried bone*

The study also highlights the need for further exploration of substrate variability and the conditions creating reduction atmospheres. Although only two substrate conditions were tested, results provide predictions for other environmental factors affecting subsurface bone alteration and a baseline to consider the extent of damage possible in actualistic fires. For instance, the thermal footprint of a fire feature that matches the degree of bone damage observed here would need to be at least ~ 20 cm in diameter, reach a temperature of 950 °C, and last for a minimum of 6 h. While ethnoarchaeological evidence shows that fires of this length occur (Mallol et al., 2007; Mallol & Henry, 2017), such high-intensity fires which can be consistently held at an extreme elevated temperature are expected to be less common in pre-industrial contexts. By reaching and sustaining damage at this extreme, however, this study suggests a maximum threshold of likely thermal alteration to faunal remains in buried substrates. Through the results of this study, it can be predicted that calcined samples would be rare at depths of −6 cm beneath a feature, except in cases where the feature is of long duration and sustained at temperatures exceeding 900 °C.

When considering larger fires, such as the Middle Paleolithic combustion features at Roc de Marsal (SW France), which span 30–130 cm (Aldeias et al., 2012), it is likely the larger footprint would result in a proportionally wider thermal impact on underlying sediments compared to the smaller feature tested here. To scale the effects of this study, we do recognize that fire temperatures must be held for a minimum of

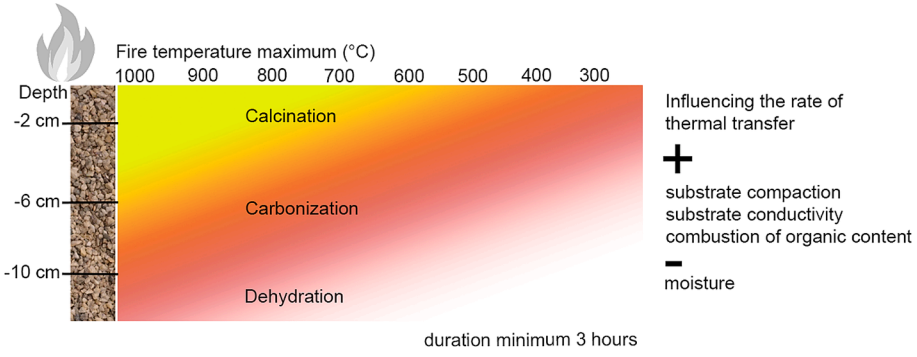

Fig. 17. Predicted degree of heat alteration for fresh bone buried directly beneath a fire event or combustion feature in dry, oxygen-accessible substrates. This figure illustrates the expected burning stages—corresponding to dehydration, decomposition (carbonization), and fusion/inversion (calcination)—based on results from this study, which sustained temperatures of 950 °C for 6 h, plus heating and cooling periods. These projections apply specifically to bones positioned directly under fire features, as both this experiment and prior research show that horizontal heat distribution diminishes significantly with distance. Factors that increase the rate of thermal transfer—and therefore the extent or duration of heat exposure—include compacted substrates, substrates with high heat conductivity, and possibly the combustion of buried organic matter. Conversely, factors that limit heat transfer include the presence of moisture, particularly in the initial stages. A minimal duration for this extent of damage is estimated at 2–3 h. Longer exposure times are expected to progressively raise sediment temperatures closer to the surface temperature, ultimately increasing the degree of heat exposure as a function of time and temperature equilibrium.

approximately three hours for heat distribution to fully penetrate the underlying sediment (Fig. 17). Future research in both experimental and archaeological settings can further investigate the impact of footprint size and heat directionality on substrates and buried materials to further document this relationship.

While this study found minimal differences between the two substrates tested and no evidence of reduction burning atmospheres, other sediments—particularly those rich in humic content—may significantly alter oxygen availability and affect bone heating. Organic material in soils could initially reduce heat transfer as moisture evaporates, but once combusted, it could increase the thermal impact on surrounding sediments (Aldeias et al., 2016). These findings underscore the need for further investigation into substrate variability and the conditions that produce reduction atmospheres under combustion features.

Bone condition and diagenetic status are expected to have a minor effect on the overall outcomes of thermal alteration. Dry, weathered bone, which has previously lost moisture, may potentially undergo dehydration more rapidly than fresh bone, but the high energy needed for the calcination of bone remains necessary (Gamelas and Martins, 2015; Han et al., 2016). The chemical and structural variability in non-stoichiometric bioapatite is unlikely to drastically alter interpretations of burning stages—dehydration, decomposition, or calcination. Fresh bones with adhering flesh and marrow may increase the heating temperature, as the organic material can act as fuel after an initial delay in temperature transfer. However, more research is needed to quantify this effect.

For scenarios in which buried bones are re-heated by above ground fire, we expect that the heat induced alterations would continue to impact the bioapatite portion of bone material. This scenario is likely to occur where combustion feature locations have been reused over multiple periods. Brief re-heating scenarios, consisting of two 30-minute heating intervals with complete cooling between exposures, did not result in any significant changes to crystal shape or size (Gallo et al., 2021).The detection of this duration of accumulated heating is also complicated, as there is not a single signal that can be used to evaluate this metric. For bones thermally altered at temperatures under calcination, one macroscopic indicator is a pale color that deviates from the typical coloration schemes described for burned bones. However, there are many misleading colorations possible, which complicates interpretations based only on visual cues (Bradfield, 2018; Dupras and Schultz, 2014; Gallo et al., 2023; Pollock et al., 2018; Reidsma et al., 2016). The deceptive coloring documented here further emphasizes that coloration is an unreliable indicator of the degree of structural and chemical alteration, and inferences should be supported whenever possible with spectroscopic analyses (Gallo et al., 2023).

At temperatures that accompany calcination, analyzing the average crystallite size of bioapatite (or, potentially at high temperatures, β-TCP) crystals may offer insights into the relationship between temperature and duration. Experimental data suggests that prolonged durations lead to larger average crystallite sizes compared to bones burnt at the same temperature but for shorter durations (Gallo et al., 2023). Additionally, the role of the OH signal at $\sim$ 3572 cm^{-1} in FTIR-ATR spectra of thermally altered bone may provide complementary information regarding bones exposed to long temperature durations but prior to calcination and will be explored further in future research.

4.2. Archaeological interpretations

The archaeological significance of thermally altered bones lies in their potential to inform hypotheses about ancient fire use. As burned bone fragments are often located in the screened materials from excavations due to their mechanical fragility, based on the findings of this study we recommend that complementary data regarding thermal alteration from the fine fraction be integrated into studies of larger faunal when possible. Further, sampling burned contexts when recognized in the field with micromorphological techniques can supply complementary evidence which preserves stratigraphic integrity. Therefore, micromorphological samples can provide contextual data on the relationship between the burned contexts and material potentially buried underneath. The framework of the microcontextual approach can be implemented in such scenarios as an interdisciplinary bridge between the geoarchaeological data in micromorphological slides and the fauna recovered in larger units through excavation. This strategy can contextualize how bone fragments are related to specific microstratigraphic units, such as those that can be identified as known components of combustion features (Goldberg et al., 2017; Mallol et al., 2013; 2017).

Despite the potential for fire to alter buried material, bones remain a valuable metric for interpreting archaeological fires. Even if bones are incidentally affected by fire rather than intentionally burned, they still provide information on the properties of the fire event which impacted them. Researchers must only remain cautious regarding if this faunal material is the result of natural or anthropogenic fire, or an intentional inclusion of fire features- such as for fuel or as a waste management strategy, or incidentally burned under a fire. Overall, thermally altered bone remains a crucial dataset for understanding ancient fire use and its broader behavioral implications, and we expect that the inferential power of thermally altered bone will increase as researchers continue to test various conditions and refine their expectations.

5. Conclusion

This experiment provides controlled data on the thermal alteration of bones under specific high-temperature conditions, offering a foundational framework for guiding future experimental and archaeological research. By testing two substrate types (gravel, and gravel and fine sand) at burial depths of –2, –6, and –10 cm, the study demonstrated the critical role of burial depth, substrate composition, and proximity to heat sources in determining the extent of thermal modification. Fully calcined bones were observed at –2 cm, while only one bone of each experimental condition calcined at –6 cm, and carbonization dominated at –10 cm. Further, pale grey and beige toned bones that can be mistaken visually for calcined bone but without the structural and chemical changes that accompany true calcination were also recorded primarily at −6 cm, providing further evidence for the importance of duration times in the interpretation of thermally altered bone coloration. These results underscore that even small variations in burial depth significantly influence subsurface bone material.

The experiment further highlights the importance of proximity to the heat source, as centrally placed samples generally experienced more intense thermal effects than peripheral ones at the same depth. This is further supported by the thermocouple data, which recorded a dramatic temperature range only 10 cm apart at the same depth, with this variation being more pronounced at the −6 cm depth than at −10 cm. Additionally, future work could explore this relationship more closely; for instance, in the case of FS1 −6 cm depth, one peripheral sample reached a higher temperature than any central sample, potentially due to shifting sediment infill. Controlling this variable more tightly in future experiments would provide deeper insights into this dynamic. Substrate composition also influenced thermal conductivity, with gravel exhibiting slightly higher heat transfer than fine sand. While spectroscopic analyses found no evidence of reducing atmospheres, the adherence of greasy residues in some cases points to the need for further study into the effects of volatile compounds released during combustion.

These findings underline the value of controlled experiments in isolating key variables that shape the thermal impact on buried materials. While the controlled nature of this study introduces some limitations in realism, such an approach is essential for building a robust understanding of the key dynamics influencing the thermal alteration of subsurface bone and emphasize reproducibility by using standardized bone samples and temperatures. The results under these laboratory conditions can inform predictive models that can later be tested under more complex and realistic conditions.

Future research should expand on this baseline by incorporating a wider range of variables, including diverse substrate types, varying moisture levels, extended and shortened exposure durations, and experiments at intermediate temperatures (e.g., 200–600 °C) that more closely mimic archaeological fire scenarios. Incorporating reheating conditions and studying more heterogeneous bone assemblages could further refine our understanding of the thermal dynamics of buried remains.

The integration of microcontextual approaches with spectroscopic analyses and visual observations remains crucial for advancing interpretations of ancient fire use. Thermally altered bones continue to provide invaluable data for reconstructing human fire using behaviors including fire construction, maintenance, and reuse. By combining controlled studies with archaeological analogues, researchers can achieve a more nuanced understanding of the complex interplay between fire, sediment, and buried materials in ancient contexts.

CRediT authorship contribution statement

Giulia Gallo: Writing – original draft, Visualization, Validation, Software, Resources, Project administration, Methodology, Investigation, Funding acquisition, Formal analysis, Data curation, Conceptualization. **Vera Aldeias:** Writing – review & editing, Validation, Supervision, Project administration. **Mareike Stahlschmidt:** Writing – review & editing, Supervision, Resources, Project administration, Methodology, Investigation, Conceptualization.

Acknowledgements

We wish to extend our sincere gratitude to Drs. Ushakov and Navrotsky (Arizona State University) for their generous provision of the XRD data, as well as to Dr. Parikh (UC Davis) for the invaluable assistance providing access to the FTIR instrument. We are also deeply appreciative of Uwe Lippmann from the Veterinärmedizinische Fakultät der Universität Leipzig for his significant assistance in sample preparation, as well as to Drs. Smith, Pederzani, Dogandžic, and Lauer for general project support at the time of experimentation. This project was made possible due to funding through the Leakey Foundation and the resources of the Max Planck Institute for Evolutionary Anthropology.

Appendix A. Supplementary material

Supplementary data to this article can be found online at https://doi.org/10.1016/j.jasrep.2025.105080.

Data availability

Data will be made available on request.

New data generated for this project is included in the supplemental materials.

References

Aldeias, V., Dibble, H.L., Sandgathe, D., Goldberg, P., McPherron, S.J., 2016. How heat alters underlying deposits and implications for archaeological fire features: a controlled experiment. J. Archaeol. Sci. 67, 64–79.

Aldeias, V., 2017. Experimental approaches to archaeological fire features and their behavioral relevance. Curr. Anthropol. 58, S191–S205. https://doi.org/10.1086/691210.

Bellomo, R.V., 1993. A methodological approach for identifying archaeological evidence of fire resulting from human activities. J. Archaeol. Sci. 20 (5), 525–553.

Bellomo, R.V., 1994. Methods of determining early hominid behavioral activities associated with the controlled use of fire at FxJj 20 Main, Koobi Fora Kenva. J. Hum. Evol. 27 (1–3), 173–195.

Bennett, J.L., 1999. Thermal alteration of buried bone. J. Archaeol. Sci. 26 (1), 1–8.

Black, S.L., Thorns, A.V., 2014. Hunter-gatherer earth ovens in the archaeological record: fundamental concepts. Am. Antiq. 79 (2), 204–226.

Bradfield, J., 2018. Some thoughts on bone artefact discolouration at archaeological sites. J Archaeol Sci Rep 17, 500–509.

Bruno, T.J., 1999. Sampling accessories for infrared spectrometry. Appl Spectrosc Rev 34 (1–2), 91–120.

Canti, M. G., & Linford, N. (2000, January). The effects of fire on archaeological soils and sediments: temperature and colour relationships. In Proceedings of the prehistoric society (Vol. 66, pp. 385-395). Cambridge University Press.

Chazan, M., 2017. Toward a long prehistory of fire. Curr. Anthropol. 58 (S16), S351–S359.

De Graaff, G., 1961. Gross effects of a primitive hearth on bones. South African Archaeol. Bull. 25–26.

Drouet, C., Aufray, M., Rollin-Martinet, S., Vandecandelaère, N., Grossin, D., Rossignol, F., Rey, C., 2018. Nanocrystalline apatites: The fundamental role of water. Am. Mineral. 103 (4), 550–564.

Dupras, T.L., Schultz, J.J., 2014. Taphonomic bone staining and color changes in forensic contexts. In: Pokines, J., Symes, S. (Eds.), Manual Forensic Taphonomy. CRC Press, Boca Raton, pp. 315–340.

Ellingham, S.T., Thompson, T.J., Islam, M., Taylor, G., 2015. Estimating temperature exposure of burnt bone—A methodological review. Sci. Justice 55 (3), 181–188.

Etok, S.E., Valsami-Jones, E., Wess, T.J., Hiller, J.C., Maxwell, C.A., Rogers, K.D., Woodgate, S.L., 2007. Structural and chemical changes of thermally treated bone apatite. J Mater Sci 42 (23), 9807–9816.

Friesem, D.E., Lavi, N., Madella, M., Boaretto, E., Ajithparsad, P., French, C., 2017. The formation of fire residues associated with hunter-gatherers in humid tropical environments: A geo-ethnoarchaeological perspective. Quat. Sci. Rev. 171, 85–99.

Gallo, G., Fyhrie, M., Paine, C., Ushakov, S.V., Izuho, M., Gunchinsuren, B., Navrotsky, A., 2021. Characterization of structural changes in modern and archaeological burnt bone: Implications for differential preservation bias. PLoS One 16 (7), e0254529.

Gallo, G., Ushakov, S.V., Navrotsky, A., Stahlschmidt, M.C., 2023. Impact of prolonged heating on the color and crystallinity of bone. Archaeol. Anthropol. Sci. 15 (9), 143.

Gamelas, J.A.F., Martins, A.G., 2015. Surface properties of carbonated and non-carbonated hydroxyapatites obtained after bone calcination at different temperatures. Colloids Surf A Physicochem Eng Asp 478, 62–70.

Gibson, I.R., Rehman, I., Best, S.M., Bonfield*, W., 2000. Characterization of the transformation from calcium-deficient apatite to β-tricalcium phosphate. J. Mater. Sci. - Mater. Med. 11, 533–539.

Goldberg, P., Miller, C.E., Mentzer, S.M., 2017. Recognizing fire in the Paleolithic archaeological record. Curr. Anthropol. 58 (S16), S175–S190.

Gowlett, J.A., Harris, J.W., Walton, D., Wood, B.A., 1981. Early archaeological sites, hominid remains and traces of fire from Chesowanja. Kenya. Nature 294 (5837), 125–129.

Gowlett, J.A., 2016. The discovery of fire by humans: a long and convoluted process. Philos. Trans. R. Soc., B 371 (1696), 20150164.

Han, Z., Mu, Z., Yin, W., Li, W., Niu, S., Zhang, J., Ren, L., 2016. Biomimetic multifunctional surfaces inspired from animals. Adv. Colloid Interface Sci. 234, 27–50.

Hoare, S., Preysler, J.B., Kabukcu, C., Kamper, T.E., Sinclair, A.G.M., Navas, C.T., 2023. There's no smoke without fire: A deep time perspective on the effects of fires on air quality, human health and habitability in the Palaeolithic and prehistory. J. Archaeol. Sci. Rep. 52, 104261.

Hollund, H.I., Ariese, F., Fernandes, R., Jans, M.M.E., Kars, H., 2013. Testing an alternative high-throughput tool for investigating bone diagenesis: FTIR in attenuated total reflection (ATR) mode. Archaeometry 55 (3), 507–532.

Krap, T., 2022. Cremains, what remains: Heat induced changes of bio-physical properties of human bone, introducing new parameters and concepts for forensic anthropological analysis. Gompel&svacina.

Mallol, C., Marlowe, F.W., Wood, B.M., Porter, C.C., 2007. Earth, wind, and fire: ethnoarchaeological signals of Hadza fires. J. Archaeol. Sci. 34 (12), 2035–2052.

Mallol, C., Hernández, C.M., Cabanes, D., Sistiaga, A., Machado, J., Rodríguez, Á., Galván, B., 2013. The black layer of Middle Palaeolithic combustion structures. Interpretation and archaeostratigraphic implications. J. Archaeol. Sci. 40 (5), 2515–2537.

Mallol, C., Henry, A., 2017. Ethnoarchaeology of Paleolithic fire: methodological considerations. Curr. Anthropol. 58 (S16), S217–S229.

Mallol, C., Mentzer, S.M., 2017. Contacts under the lens: Perspectives on the role of microstratigraphy in archaeological research. Archaeol. Anthropol. Sci. 9, 1645–1669.

Mamede, A.P., Gonçalves, D., Marques, M.P.M., Batista de Carvalho, L.A., 2018a. Burned bones tell their own stories: A review of methodological approaches to assess heat-induced diagenesis. Appl. Spectrosc. Rev. 53 (8), 603–635.

Mamede, A.P., Vassalo, A.R., Piga, G., Cunha, E., Parker, S.F., Marques, M.P.M., Gonçalves, D., 2018b. Potential of bioapatite hydroxyls for research on archeological burned bone. Anal. Chem. 90 (19), 11556–11563.

Martin, R.B., Burr, D.B., Sharkey, N.A., Fyhrie, D.P., 2015. Skeletal Tissue Mechanics. Springer.

Marques, M.P., Gonçalves, D., Mamede, A.P., Coutinho, T., Cunha, E., Kockelmann, W., Batista de Carvalho, L.A.E., 2021. Profiling of human burned bones: oxidising versus reducing conditions. Sci. Rep. 11 (1), 1361.

Mayne Correia, P., 1997. Fire modification of bone: a review of the literature. In: Sorg, M., Haglund, W. (Eds.), Forensic Taphonomy: the Postmortem Fate of Human Remains. CRC Press, Boca Raton, pp. 275–293.

Munsell Color (Firm) (2010) Munsell soil color charts : with genuine Munsell color chips. Grand Rapids, MI :Munsell Color.

Nakamoto, K., 2009. Infrared and Raman spectra of inorganic and coordination compounds, part B: applications in coordination, organometallic, and bioinorganic chemistry. John Wiley & Sons.

Patonai, Z., Maasz, G., Avar, P., Schmidt, J., Lorand, T., Bajnoczky, I., Mark, L., 2013. Novel dating method to distinguish between forensic and archeological human skeletal remains by bone mineralization indexes. Int. J. Leg. Med. 127, 529–533.
Piga, G., Amarante, A., Makhoul, C., Cunha, E., Malgosa, A., Enzo, S., & Gonçalves, D. (2018). Research Article β-Tricalcium Phosphate Interferes with the Assessment of Crystallinity in Burned Skeletal Remains.
Pollock, C.R., Pokines, J.T., Bethard, J.D., 2018. Organic staining on bone from exposure to wood and other plant materials. Forensic Sci Int 283, 200–210.
Reidsma, F.H., van Hoesel, A., van Os, B.J., Megens, L., Braadbaart, F., 2016. Charred bone: Physical and chemical changes during laboratory simulated heating under reducing conditions and its relevance for the study of fire use in archaeology. J. Archaeol. Sci. Rep. 10, 282–292.
Reidsma, F.H., 2022. Laboratory-based experimental research into the effect of diagenesis on heated bone: implications and improved tools for the characterisation of ancient fire. Sci. Rep. 12 (1), 17544.
Rey, C., Combes, C., Drouet, C., Glimcher, M.J., 2009. Bone mineral: update on chemical composition and structure. Osteoporos Int 20 (6), 1013–1021.
Rietveld, H.M., 1969. A profile refinement method for nuclear and magnetic structures. J Appl Crystallogr 2 (2), 65–71.
Shahack-Gross, R., Bar-Yosef, O., Weiner, S., 1997. Black-coloured bones in Hayonim Cave, Israel: differentiating between burning and oxide staining. J Archaeol Sci 24 (5), 439–446.
Shehata, T.P., Krap, T., 2024. An overview of the heat-induced changes of the chemical composition of bone from fresh to calcined. Int. J. Leg. Med. 138 (3), 1039–1053.
Snoeck, C., Lee-Thorp, J.A., Schulting, R.J., 2014. From bone to ash: Compositional and structural changes in burned modern and archaeological bone. Palaeogeogr. Palaeoclimatol. Palaeoecol. 416, 55–68.
Snoeck, C., Schulting, R.J., Lee-Thorp, J.A., Lebon, M., Zazzo, A., 2016. Impact of heating conditions on the carbon and oxygen isotope composition of calcined bone. J. Archaeol. Sci. 65, 32–43.
Stahlschmidt, M.C., Miller, C.E., Ligouis, B., Hambach, U., Goldberg, P., Berna, F., Conard, N.J., 2015. On the evidence for human use and control of fire at Schöningen. J. Hum. Evol. 89, 181–201.
Stahlschmidt, M.C., Mentzer, S.M., Heinrich, S., Cooper, A., Grote, M.N., McNeill, P.J., Wilder, J.C., Steele, T.E., 2023. Impact of a Recent Wildfire on Tortoises at Cape Point, South Africa, and Implications for the Interpretation of Heated Bones in the Archaeological Record. Archaeol Anthropol Sci. https://doi.org/10.1007/s12520-023-01806-4.
Steele, T.E., Gallo, G., Martisius, N.L., 2025. Animal resources in experimental archaeology: a reflection on standards and ethics. J. Archaeol. Sci. Rep. 61, 104901.
Stiner, M.C., Kuhn, S.L., Weiner, S., Bar-Yosef, O., 1995. Differential burning, recrystallization, and fragmentation of archaeological bone. J. Archaeol. Sci. 22 (2), 223–237.
Téllez, E., Saladié, P., Pineda, A., Marín, J., Vallverdú, J., Chacón, M.G., Carbonell, E., 2022. Incidental burning on bones by Neanderthals: the role of fire in the Qa level of Abric Romaní rock-shelter (Spain). Archaeol. Anthropol. Sci. 14 (6), 119.
Thompson, T., 2004. Recent advances in the study of burned bone and their implications for forensic anthropology. Forensic Sci Int 146, S203–S205.
Thompson, T.J.U., Gauthier, M., Islam, M., 2009. The application of a new method of Fourier Transform Infrared Spectroscopy to the analysis of burned bone. J Archaeol Sci 36 (3), 910–914.
Toby, B.H., Von Dreele, R.B., 2013. GSAS-II: the genesis of a modern open-source all purpose crystallography software package. J Appl Crystallogr 46, 544–549.
Turner, E., Hutson, J., Villaluenga, A., García Moreno, A., Gaudzinski-Windheuser, S., 2018. Bone staining in waterlogged deposits: a preliminary contribution to the interpretation of near-shore find accumulation at the Schöningen 13II-4 'Spear-Horizon'site. Lower Saxony. Germany Histor Biol 30 (6), 767–773.
van Hoesel, A., Reidsma, F.H., van Os, B.J., Megens, L., Braadbaart, F., 2019. Combusted bone: Physical and chemical changes of bone during laboratory simulated heating under oxidising conditions and their relevance for the study of ancient fire use. J. Archaeol. Sci. Rep. 28, 102033.
Weiner, S., Bar-Yosef, O., 1990. States of preservation of bones from prehistoric sites in the Near East: a survey. J Archaeol Sci 17 (2), 187–196.
Wrangham, R., 2017. Control of fire in the Paleolithic: evaluating the cooking hypothesis. Curr. Anthropol. 58 (S16), S303–S313.
Wrangham, R., 2009. Catching fire: how cooking made us human. Basic books.
Zazzo, A., Saliege, J.F., Person, A., Boucher, H., 2009. Radiocarbon dating of calcined bones: where does the carbon come from? Radiocarbon 51 (2), 601–611.
Zhang, G., Deng, X., Guan, F., Bai, Z., Cao, L., Mao, H., 2018. The effect of storage time in saline solution on the material properties of cortical bone tissue. Clin. Biomech. 57, 56–66.

Further reading

Buikstra, J.E., Swegle, M., 1989. Bone modification due to burning: experimental evidence. In: Bonnichsen, R., Sorg, M. (Eds.), Bone Modification, Center for the Study of the First Americans, Institute for Quaternary Studies. University of Main, Ororo, pp. 247–258.